Electron Response of STEREO High Energy Telescope Through GEANT4 Modeling

Daniel Y. Lo
Mentors: Mark E. Wiedenbeck, Edward C. Stone
Space Radiation Laboratory, California Institute of Technology, Pasadena, CA 91125, USA.

Abstract

Accurate measurements of solar electron energies and fluxes are crucial in understanding the processes that accelerate solar energetic particles and drive space weather. Using GEANT4 libraries, we developed an instrument model for the High Energy Telescope (HET) on the Solar TErrestrial RElations Observatory (STEREO) to study its electron response. Such a theoretical calibration is required to translate observations into a quantitative description of the distribution of solar electron energies. Using the model, we also studied the effects of the instrument housing on the electron response, and these findings help inform better instrument designs for future sensors to optimize the quality of the electron measurements.

1 Introduction

We live in the extended atmosphere of an active star. While this star is the primary ultimate source of energy that supports all life on Earth, it can at times produce streams of high energy particles and radiation that can instead harm life. Fortunately, for most of history, terrestrial life has been protected by the Earth's magnetic field and atmosphere. However, as we continue to make advances in this space age, the protection offered by the Earth's magnetic field and atmosphere is no longer sufficient. Already, strong solar energetic particle (SEP) events can in some cases disrupt our power grids and cripple our satellite systems. Manned space missions to near-Earth asteroids in the future will take astronauts completely outside Earth's magnetic field. Just as it is important to understand how the Sun powers terrestrial weather, it is also critical for us to appreciate the effects of various solar processes on space weather and be able to take the appropriate measures to mitigate the risks associated with potentially dangerous solar events. However, these solar processes are currently not well understood. The mechanisms of energetic particle acceleration from SEP events are still being elucidated, with no single model being widely accepted and sufficiently well-developed to have any significant predictive power. A good description of the electron energy distributions is critical in providing constraints and informing refinements for the current models (e.g. Reames [1] and Guo and Giacalone [2]).

To this end, NASA's Solar Terrestrial Probes (STP) program was started to address fundamental questions about the physics of space plasmas and the flow of mass and energy through the solar system [3]. Launched in 2006, the Solar TErrestrial RElations Observatory (STEREO) mission, the third of five in the STP program, employs two nearly identical space-based observatories to study the Sun and the nature of its coronal mass ejections (CMEs) [4]. One of the spacecraft is ahead of Earth in its orbit, while the other trails the Earth, allowing the first simultaneous three-dimensional observations of CMEs and the ambient solar corona and heliosphere. The High Energy Telescope (HET), as part of the In-Situ Measurements of Particles and CME Transients (IMPACT) payload on each of the spacecraft, is designed to measure SEP energies and fluxes [5]. Previous studies have found correlations between electrons below 0.5 MeV and protons below 10 MeV from SEP events (Haggerty and Roelof [6] and Cliver [7]), and the ability of the HET to measure electrons up to 6 MeV makes it well-suited to extend these correlation relationships to higher

energies. Ultimately, a good description of the relative energy distributions of electrons and heavier particles would allow us to provide improved forecasts of the intensity and timing of SEP events. In a strategy similar to that adopted in earthquake warning systems, higher-velocity electrons released by SEP events at the Sun can provide us with advance notice of the slower and more destructive heavier ions that arrive at Earth about 45 minutes later.

The total energy and the rate of energy loss of the particle in the HET gives a unique signature that can then be used to identify the particle. However, the structure of this signature is much more complicated for an electron than for a proton or ion due to the electron's greater scattering off various parts of the telescope from the lower mass of the electron. This greater scattering gives rise to broader response curves associated with each energy range and more significant overlapping among them, making it more difficult to determine the incident energy and flux. Nonetheless, given suitable computational tools that are able to fully model the scattering of the electrons in a realistic instrument configuration, the HET can be calibrated despite the greater uncertainties. Only with such calibrations can we quantitatively characterize the distribution of solar electron energies. However, such a comprehensive instrument model that takes scattering into account has not yet been developed to study the electron response of the HET.

Furthermore, a calibration of the electron response of the HET may reveal insights into ways of minimizing the effects of electron scattering in space instruments to optimize the quality of the electron signal, thus informing the design of future similar particle detectors, such as the ISIS/EPI-Hi instrument on the Solar Probe+ mission, currently in Phase B (Conceptual Design) and scheduled to launch in 2018.

In this paper, we shall describe our development of an instrument model of the HET using the GEANT4 simulation toolkit, and present the results we obtained in our simulations based on the model we developed. We shall also show that, in the case of the HET, the instrument housing in fact has no significant effect on the instrument response to electrons entering through its aperture. The organization of this paper is as follows. In Section 2 the construction and operation of the HET are outlined. Section 3 introduces the GEANT4 toolkit and our instrument models, and numerical results are presented in Section 4. A discussion of the results follows in Section 5, and conclusions appear in Section 6.

2 Instrumentation

Full details of the construction of the HET can be found in the technical paper by von Rosenvinge et al. [5]. A brief summary is now presented here.

The High Energy Telescope (HET) is one of four instruments in the Solar Energetic Particle (SEP) subsystem that is part of the IMPACT (In-Situ Measurements of Particles and CME Transients) investigation on STEREO (Figure 1). Together with the other instruments in the investigation, the HET is specifically designed to address the following Science Objective in STEREO Mission Requirements Document (MRD):

> Discover the mechanisms and sites of energetic particle acceleration in the low corona and the interplanetary medium.

In particular, the HET is a multi-detector particle telescope that is capable of detecting stopping electrons from 0.7 to 6 MeV, and protons and heavier ions up to 40 MeV/nucleon.

2.1 Construction

Figure 2 shows a cross-sectional view of an assembled HET telescope. There are six sets of ion-implanted Si detectors (H1 to H6). H3, H4 and H5 each consist of two separate 1 mm thick detectors, while H2 and H6 have only one. H1 has two distinct detection areas on the same Si disk. The spacing between the bottom of the H1 detector and the top of the H2 detector is 3.68 cm. Between the remaining detectors, this spacing is 0.15 cm.

The detectors were made using planar, polygonal Si disks that were mounted in a mechanical mount constructed using printed circuit board/flex-circuit technology. The H1 detector has two separate sensitive areas on the junction side that are defined by ion implanting 2 separate p-n junctions (Figure 3). The inner

Figure 1: Photograph of HET (center left) as part of the IMPACT payload. Overall height of the full IMPACT payload shown above is about 43.4 cm. Figure is obtained from von Rosenvinge et al. [5].

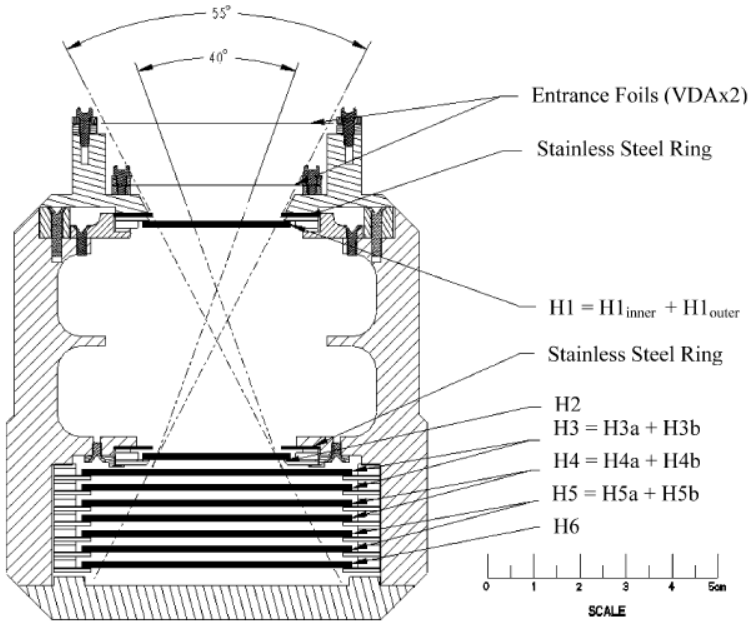

Figure 2: Schematic cross-section of the HET. Figure is obtained from von Rosenvinge et al. [5].

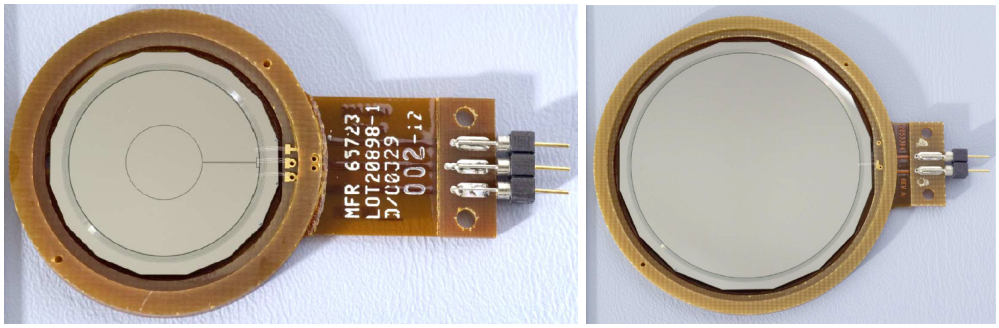

Figure 3: Junction side of the H1 detector (left) and a stack detector (right). Images are obtained from von Rosenvinge et al.[5]

sensitive area is a circle, 0.8 cm in diameter. The outer sensitive area is a concentric ring, with outer diameter 2 cm, around the inner circular area. The outer area is separated from the inner area by a circular gap that is 60 μm wide. In addition, the outer ring has a narrow (130 μm wide) radial area cut-out through which passes a narrow extension of the central area that terminates in a small pad (1 mm $\times$ 0.28 mm) located just inside of the outer circular ring. Surrounding the outer sensitive area on the junction side is a stepped guard intended to reduce excess detector leakage current. The stepped guard consists of a sequence of separate, narrow metalized rings that are allowed to float electrically.

The H2 detector is identical to the H1 detector but it has the two separate areas on the junction side electrically shorted together external to the detector mount. In effect, the H2 detector acts as a circular detector 2 cm in diameter by 1 mm thick.

The remainder of the HET telescope is constructed using a second detector type that only has a single circular p-n junction with diameter 4 cm (Figure 3). These are referred to as the stack detectors.

The telescope housing is designed to prevent external light from reaching any detector surface. The front end of the telescope is blocked by two separate Kapton foils, each 0.005" thick and coated front and back with vapor deposited aluminum (VDA). The double foil design is intended to decrease the effects of pin-holes in the VDA and also to provide better protection from incident micrometeoroids. The housing of the telescope is also designed to reduce the numbers of low energy particles that can reach any of detectors H2 through H6 without passing through H1 first. In order to minimize the background signal, not only are the walls made of 1 cm thick aluminum, 0.5 mm thick stainless steel rings with inner diameter of 21.0 mm are also included in front of H1 and H2.

2.2 Particle Identification

The HET uses the $\Delta E \times E'$ method of particle identification, where ΔE refers to the energy loss of a particle with incident kinetic energy E as it traverses a thin detector with thickness Δx, and $E' = E - \Delta E$ is the residual energy after passing through the ΔE detector. On a plot of ΔE against E' (Figure 4), particles with different charge and mass will be separated into different tracks. The location of each track depends upon the incident energy. More details about this technique is available in Goulding and Harvey[8].

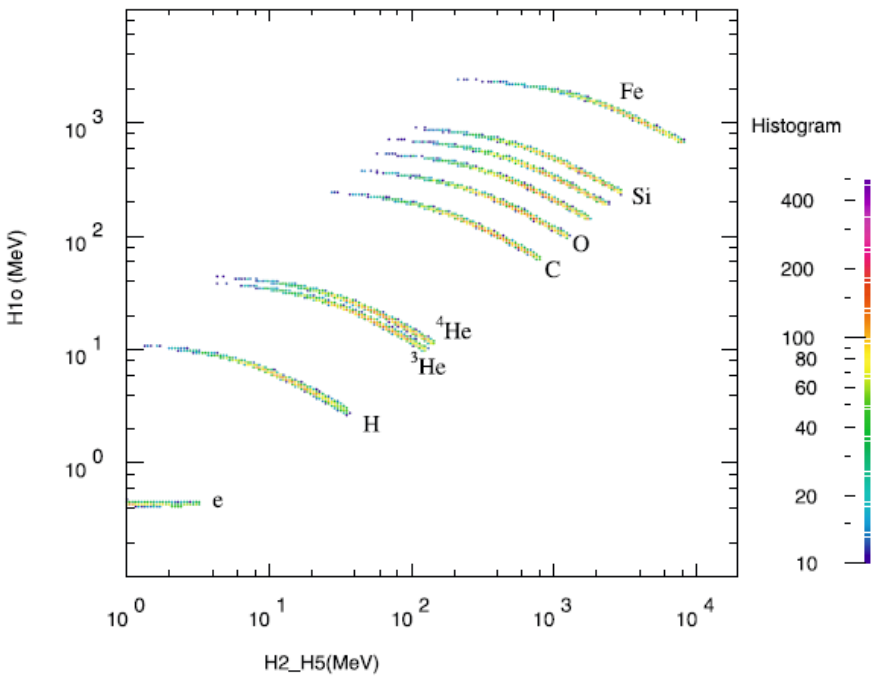

Figure 4: Simulated response of the HET telescope to various incident particles. A non-scattering model is used for electrons in this figure. Figure is obtained from von Rosenvinge et al. [5].

3 Simulation

3.1 Geometry Factor and Effective Area

The sensitivity of a telescope is commonly described in terms of its geometry factor. The geometry factor G is the proportionality factor relating the count rate C to an isotropic incident intensity I onto the telescope:

$$C = GI$$

For simple geometries and straight particle trajectories, analytical calculation of the geometry factor is feasible [9]. However, electron scattering and the more complex detector geometries of the HET means that such an analytical approach would require an immense effort. Thus in this study we shall numerically compute the geometry factor of the HET using Monte Carlo techniques according to the recipe laid out in Sullivan [9].

While the geometry factor describes the sensitivity of the telescope to an isotropic distribution of particles, it is often useful to investigate how the telescope response depends on the direction of the incident particles. Thus mirroring the definition for G, we define the effective area A:

$$C = AI_B$$

where I_B is the intensity of a particle beam incident on the telescope. Thus A depends on the incident direction of the particle beam. A and G are then related through the simple integration

$$G = \iint A \sin\theta d\theta d\phi$$

The complete formulas and numerical methods for calculating A and G in our analysis of the results are provided in Appendix A.

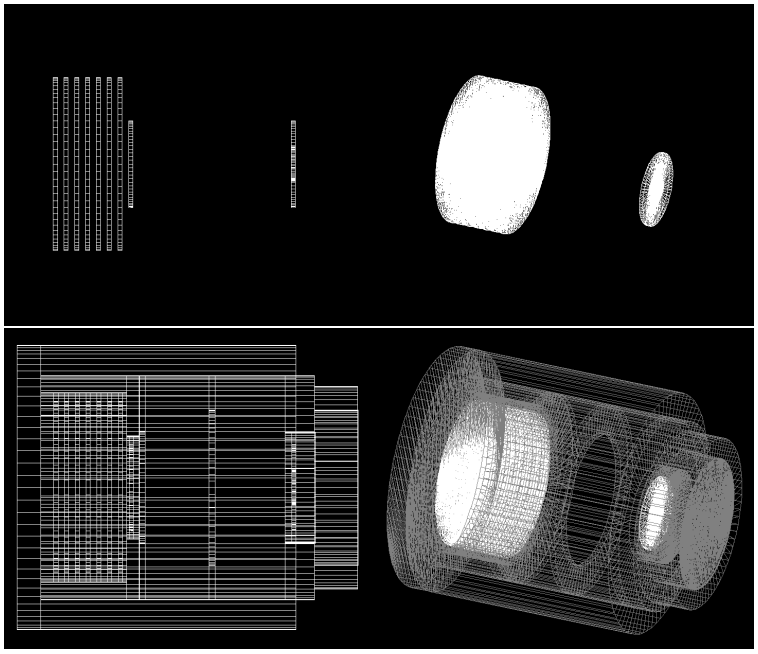

Figure 5: Side (left) and tilted (right) views of the basic (top) and full (bottom) HET models. The detectors are shown in white in the tilted models.

3.2 GEANT4

GEANT4 (GEometry ANd Tracking) is a C++ toolkit developed through an international collaboration for simulating the passage of particles through matter using Monte Carlo techniques [10]. It is widely used across many fields ranging from high-energy, nuclear and accelerator physics, to medicine and space science and engineering, including full-scale detector simulations for experiments at the Large Hadron Collider and other facilities. In addition to having a wide and active user community, the GEANT4 project benefits from continued efforts to develop and support the toolkit, including the refinement and validation of physics models. Furthermore, GEANT4 also offers a wide variety of drivers for visualizing detector geometries and particle trajectories, providing an aid to understanding the relevant physics and troubleshooting the simulation. For these reasons, GEANT4 is chosen to simulate the electron response of the HET. Specifically, GEANT 4.9.6 libraries and Microsoft Visual C++ 2010 compiler are used to build the simulation program.

3.3 Modeling and Program Design

Two specific models of the HET were used in our simulations (Figure 5). The basic model comprises only the sensitive detector elements, while the full model has the additional non-detecting elements. These non-detecting elements include the instrument housing, which we have divided into 10 distinct components (Figure 6), and the 2-mm-wide silicon rings around the detectors H1-H6. In both models, we have assumed cylindrical symmetry.

For simulations with both the basic and full models, a circular plane source was used. This source was placed at the same position in both models - just outside the outer Kapton film window of the full model. Particles were "fired" from a random point on this circular surface at a pre-determined polar angle θ and with a pre-determined incident energy E into the HET. Particle trajectories and interactions with the solids were determined by the FTFP_BERT 2.0 physics list. The FTFP_BERT physics list, recommended for applications involving particle energies less than 5 GeV, includes standard electromagnetic processes such as ionization, Compton scattering and photoelectric effect, and the Bertini cascade model for scattering

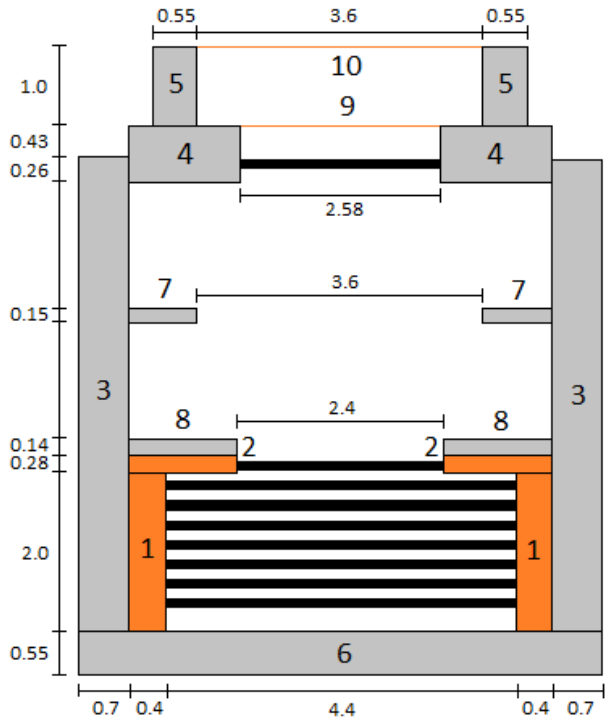

Figure 6: Schematic of full model with its 10 housing components labeled. Aluminum components are in gray, Kapton in orange and silicon in black. Dimensions (in smaller font and decimals) are in cm.

of hadrons less than 5 GeV. The energy deposited in each detector element in the HET, ΔE, was then measured using the G4PSEnergyDeposit class provided in GEANT4. In total, the simulation runs spanned θ-space from 0° to 60° in steps of 5°, and E-space from 0.6 MeV to 6 MeV in steps of 0.2 MeV. Although the calculation of the geometry factor would require us to know the effective area up to 90°, we found that the effective area becomes negligible by 60° and thus we do not expect significant contribution from higher values of θ. 5000 events are simulated for each value of θ and E, giving a total of 1,820,000 events for each model.

In addition to being able to accurately model particle scattering in the HET, the simulation program we have developed is also designed to be flexible to be used for various other simulations of the HET, and even to be fully re-adapted for use with another similiar instrument. The simulation parameters can be customized through an external macro file, allowing the user to set the energy, direction, position and type of the source particles, and the number of events for each simulation run without having to recompile the source code. The geometry of the instrument is loaded into the program via an external GDML file, which can be generated from a STEP file created from existing geometries in 3D computer-aided design (CAD) software such as SolidWorks and AutoCAD. The full procedure for this import process is described in Constantin et al.[11]. By loading in the appropriate GDML file for the new instrument, and with minor rewriting of the code to reconfigure the sensitive regions of the instrument, the program will quickly be ready for use to run simulations for a second instrument.

4 Numerical Results

Events are classified into the following types:

Total: $\mathrm{H1i} \cdot \overline{\mathrm{H1o}} \cdot \mathrm{H2}$

All Energy: $\mathrm{H1i} \cdot \overline{\mathrm{H1o}} \cdot \mathrm{H2}$, Total $\Delta E \geq E - \text{buffer}$

Ranges

R2: $\mathrm{H1i} \cdot \overline{\mathrm{H1o}} \cdot \mathrm{H2} \cdot \overline{\mathrm{H3}} \cdot \overline{\mathrm{H4}} \cdot \overline{\mathrm{H5}} \cdot \overline{\mathrm{H6}}$

R3: $\mathrm{H1i} \cdot \overline{\mathrm{H1o}} \cdot \mathrm{H2} \cdot \mathrm{H3} \cdot \overline{\mathrm{H4}} \cdot \overline{\mathrm{H5}} \cdot \overline{\mathrm{H6}}$

R4: $\mathrm{H1i} \cdot \overline{\mathrm{H1o}} \cdot \mathrm{H2} \cdot \mathrm{H3} \cdot \mathrm{H4} \cdot \overline{\mathrm{H5}} \cdot \overline{\mathrm{H6}}$

R5: $\mathrm{H1i} \cdot \overline{\mathrm{H1o}} \cdot \mathrm{H2} \cdot \mathrm{H3} \cdot \mathrm{H4} \cdot \mathrm{H5} \cdot \overline{\mathrm{H6}}$

R6: $\mathrm{H1i} \cdot \overline{\mathrm{H1o}} \cdot \mathrm{H2} \cdot \mathrm{H3} \cdot \mathrm{H4} \cdot \mathrm{H5} \cdot \mathrm{H6}$

where H indicates coincidence and $\overline{\mathrm{H}}$ indicates anti-coincidence with the H detector. Note that a particular event can be in multiple groups; in fact all groups are subsets of the Total group. No energy thresholds are set for any of the detectors, and thus any trajectory crossings will be taken into account when determining the coincidence/anti-coincidence criteria. For the All Energy events, a buffer of 0.1 keV is used with the basic model due to floating-point errors when summing for the total energy deposited, while a buffer of 61.4 keV is used with the full model both for the floating-point errors and to account for energy loss through the two Kapton windows. Thus All Energy events correspond to electrons that deposit all incident energy in the HET and eventually stop in the telescope. The R2-R5 range electrons may or may not stop in the HET, but R6 electrons are treated as having exited the instrument out the back.

4.1 Basic Model

Figure 7 directly shows the desired data product from our simulations for the basic model of the HET. For any energy measured by the HET, we can simply take a horizontal section across the contour plot. These horizontal sections, such as those shown in Figure 8, give us the exact contribution to the detected signal in terms of geometry factor by electrons at various incident energies. The middle and bottom plots in Figure 7 provide additional constraints based on the range data returned from the HET. To determine the incident

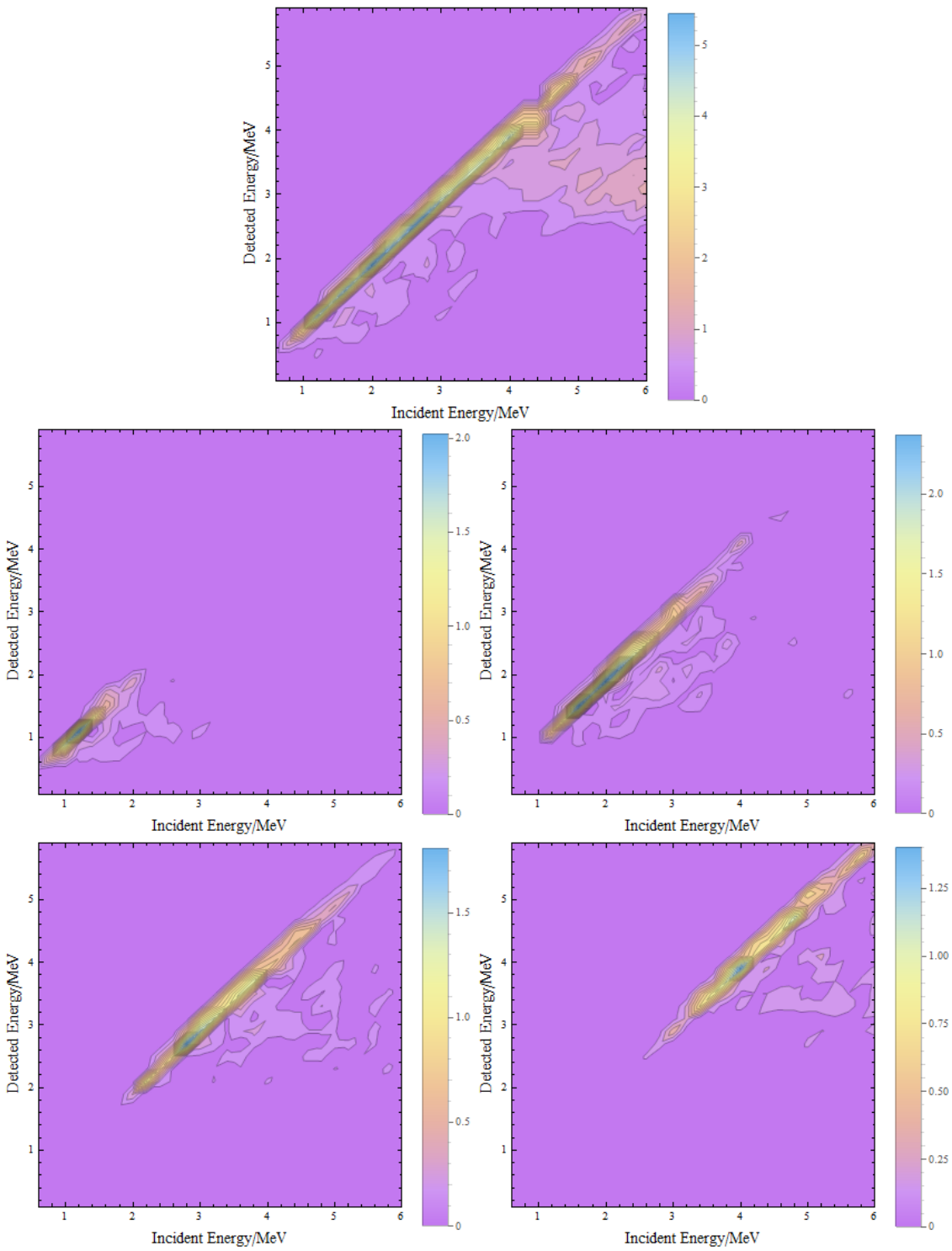

Figure 7: *Basic Model*. Geometry factors for various detected detected and incident energies in mm^2 sr. Top: Geometry factors for Total events. Contour interval is 0.3 mm^2 sr. Middle left: Geometry factors for R2 events. Middle right: Geometry factors for R3 events. Bottom left: Geometry factors for R4 events. Bottom right: Geometry factors for R5 events. Contour intervals for all range plots are 0.1 mm^2 sr.

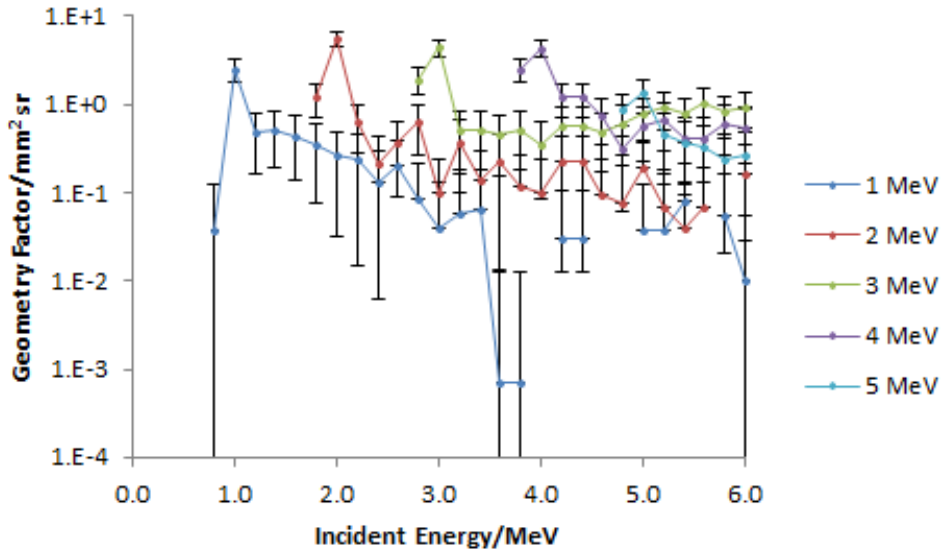

Figure 8: *Basic Model*. Sections across the Total events plot.

energy distribution, we can apply numerical variational techniques starting with a trial incident energy distribution to find the distribution that most closely matches the detected energy and range distributions based on the calibration provided in Figure 7.

Three features stand out in Figure 7. Firstly, no significant number of events in the Total category are detected below the minimum energy of 0.4 MeV required to cross H1i to reach H2 and satisfy the minimum coincidence criterion. Correspondingly, this minimum energy increases by 0.8 MeV for each subsequent range. These values agrees with the stopping power of 1.5 MeV-cm^2/g for a 1 MeV electron, or a loss of 0.4 MeV per millimeter of silicon. Secondly, a diagonal ridge cuts across the plot, corresponding to the All Energy events, suggesting that the All Energy events have the largest contribution in the probability distribution for the incident energies. Finally, there is also a horizontal ridge centered at 3.2 MeV detected energy with increasing height towards higher incident energies for the Total events, corresponding to minimum-ionizing electrons that travel straight through the instrument. Since these events do not fulfill the range criteria, the horizontal ridge does not appear in any of the range plots.

While Figure 7 is useful in an experimental setting for converting an observed electron energy spectrum to the actual electron energy spectrum, it is not as useful when studying electron scattering in the HET. Figures 9, 10 and 11 provide a clearer picture of the trajectories of electrons through the HET and the degree of scattering.

Figure 9 shows the effective area of the HET for Total events. We observe that there is a peak in effective area at $\theta = 0°$, and this peak becomes sharper at higher incident energies. This effective areas in Figure 9 are integrated to give the geometry factors plotted as the dark blue Total curve in Figure 10. The All Energy and R6 curves in Figure 10 are produced in a similar manner from the effective areas for the respective events. From the coincidence criteria, we can see that the main difference between Total events and All Energy event categories is that the latter requires electrons to stop in the HET. Thus the difference between the geometry factors corresponds to the "loss" of electrons by two processes: (1) scattering by the H2-H5 detectors out the sides and (2) loss out the end through H6. Now the loss through H6 is described by the R6 events, and thus the difference between the dark blue Total curve and the green All Energy + R6 curve reflects the degree of scattering by the H2-H5 detectors. We can see that as the incident energy of the electron increases, the degree of electron scattering, as reflected by the difference between the two curves, first increases to a broad

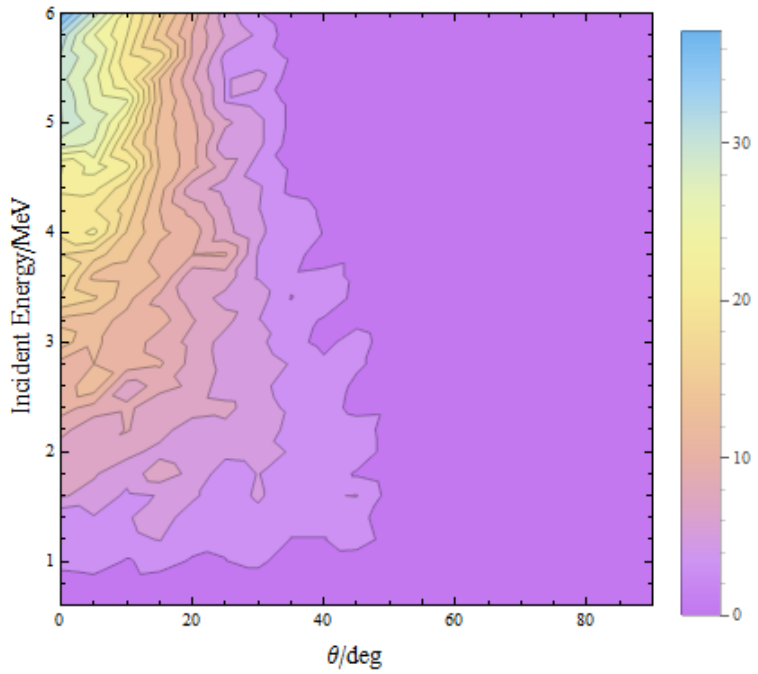

Figure 9: *Basic Model*. Contour plot of effective area of HET in mm^2 for Total events. Contour interval is 2 mm^2.

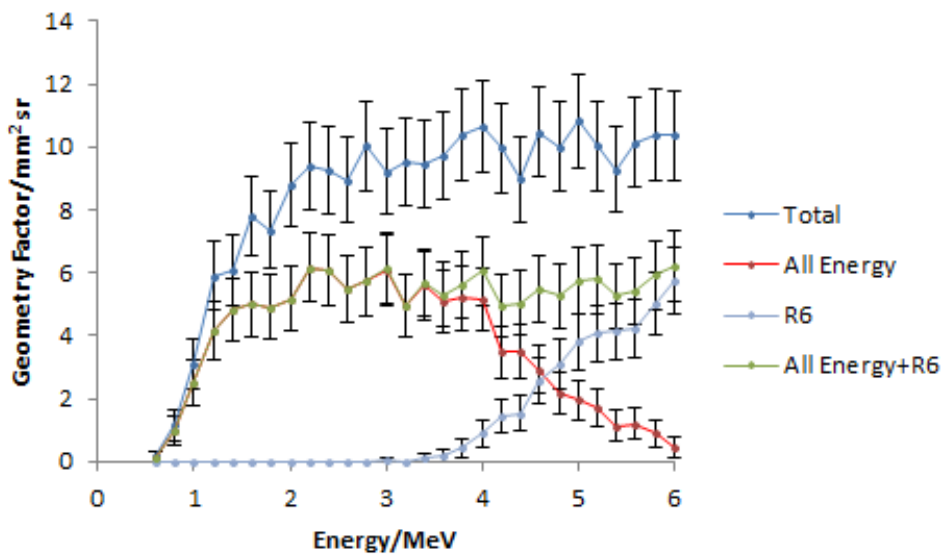

Figure 10: *Basic Model*. Geometry factors against energy for Total (dark blue), All Energy (red) and R6 (light blue) events. The green curve shows the sum of All Energy and R6 events.

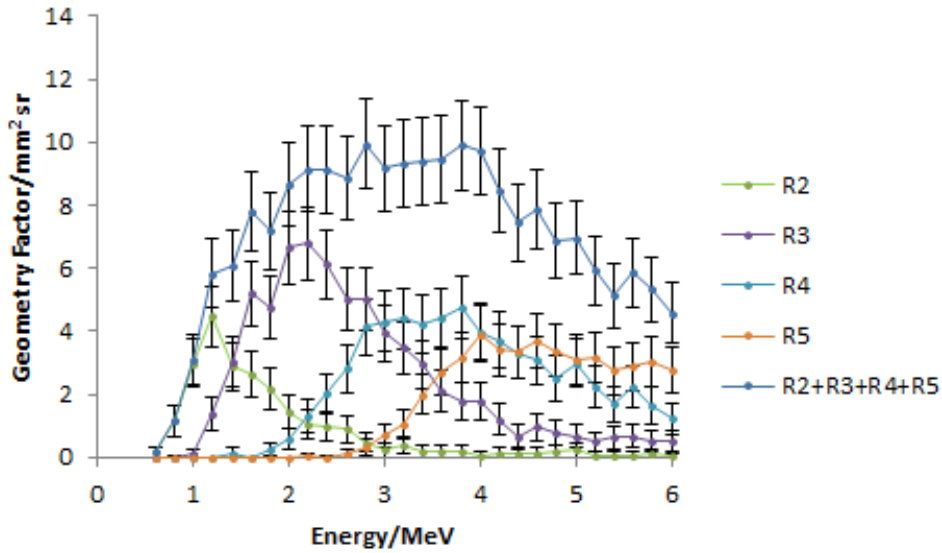

Figure 11: *Basic Model.* Geometry factors for ranges R2 to R5.

peak before decreasing slowly.

Figure 11 shows the geometry factors for electron trajectories satisfying the various range criteria. We observe that as the range becomes longer, peaks shift towards the higher incident energies, and the peak height also decreases. The R2 curve is an exception, with its peak lower than that for the R3 curve, primarily because the H2 detector is half as thick as the other detectors. H3-H5 all comprise two detectors each, while the H2 has only one, making a electron half as likely to stop in H2 than the other detectors if they were all placed at the same position.

4.2 Full Model

Figures 12, 13, 14 and 15 show the simulation results using the full model. Comparing with their counterparts for the basic model, we find that the same features still exist. From Figure 12, the "calibration" plot for the full model, we again see the diagonal ridge for the All Energy events, and the small horizontal ridge at 3.2 MeV detected energy for the straight-through electrons. The minimum required energies for the Total events and the various ranges apply for the full model as well. Figure 13 is the plot of effective area for the Total events with the full model, and we see the same peak at $\theta = 0°$, narrowing towards higher incident energies. In Figure 14, the full model version for Figure 10 shown earlier, we see a similar initial rapid increase and then plateau in geometry factor for Total events, and R6 events start to climb steadily from 3 MeV. The relative heights and positions of the peaks for the various ranges in Figure 15 are the same as in Figure 11.

Figure 16 compares some of the important geometry factors calculated based on the two models. The full model has slightly larger geometry factors compared to the basic model for both the Total and the R6 events. However, the reverse seems to be the case for the All Energy events. This, however, may not be a true feature, and can simply be due to electrons having to pass through two additional Kapton windows before reaching the H1i detector in the full model. While we have attempted to account for the energy loss in the Kapton with a different value for the buffer, the value we have selected is the energy loss by an electron travelling normal to the windows, thus corresponding to the minimum energy loss. The actual energy loss through the two windows is larger, making it appear as though there are less electrons depositing all their energy in the detectors after passing through the windows, and thus resulting in lower calculated geometry

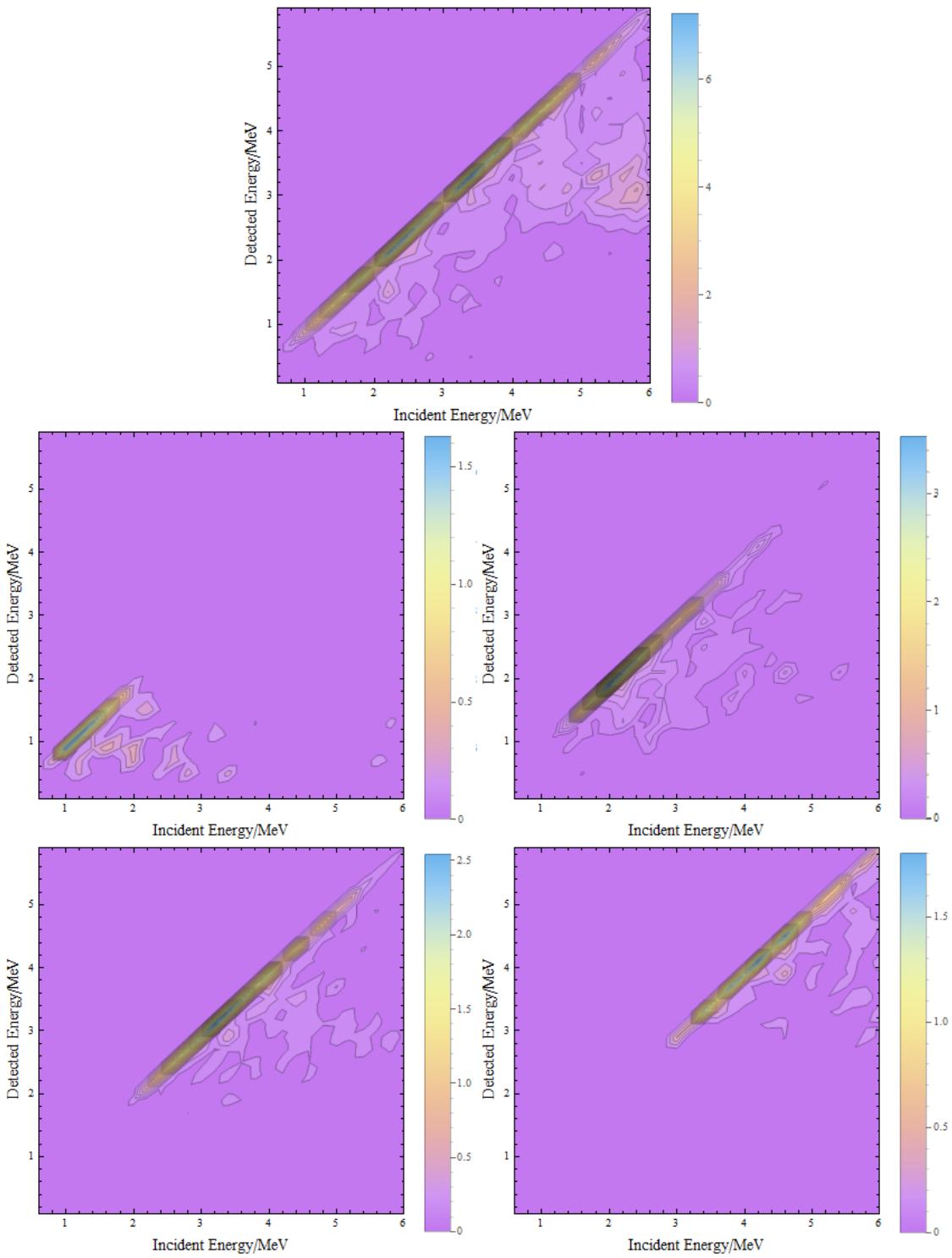

Figure 12: *Full Model*. Geometry factors for various detected detected and incident energies in mm^2 sr. Top: Geometry factors for Total events. Contour interval is 0.3 mm^2 sr. Middle left: Geometry factors for R2 events. Middle right: Geometry factors for R3 events. Bottom left: Geometry factors for R4 events. Bottom right: Geometry factors for R5 events. Contour intervals for all range plots are 0.1 mm^2 sr.

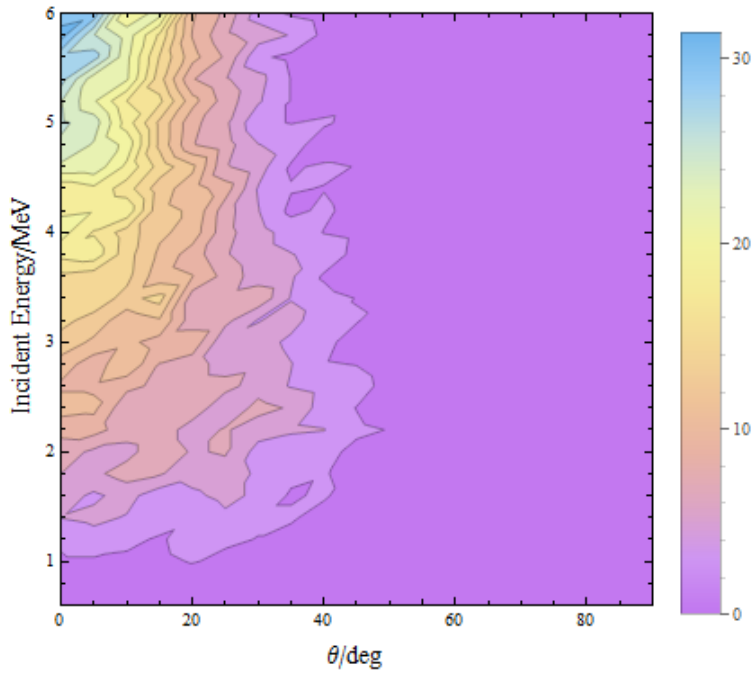

Figure 13: *Full Model*. Contour plot of effective area of HET in mm^2 for Total events. Contour interval is 2 mm^2.

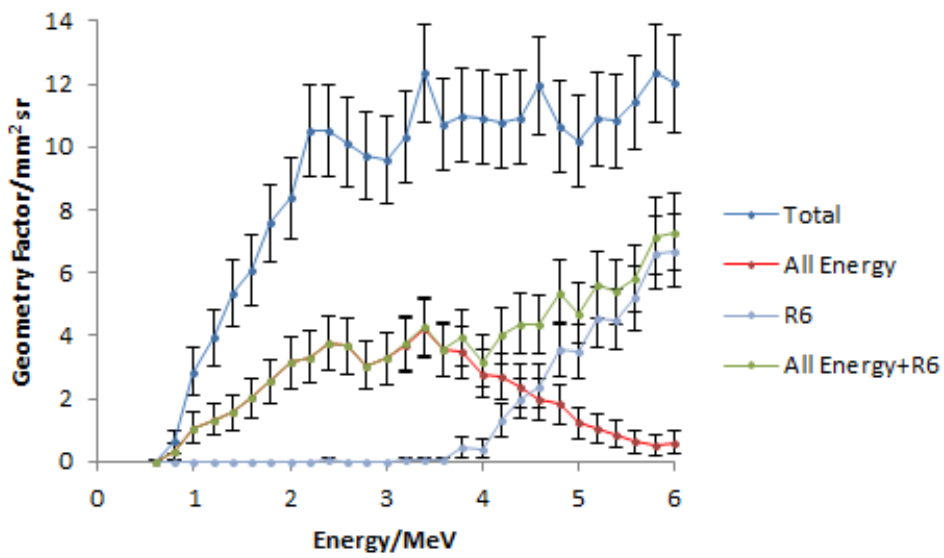

Figure 14: *Full Model*. Geometry factors against energy for Total (dark blue), All Energy (red) and R6 (light blue) events. The green curve shows the sum of All Energy and R6 events.

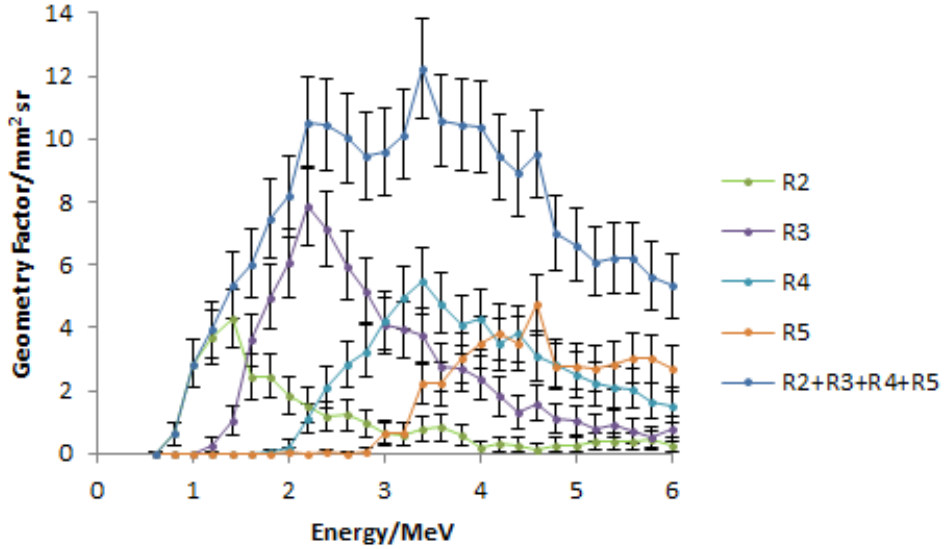

Figure 15: *Full Model*. Geometry factors for ranges R2 to R5.

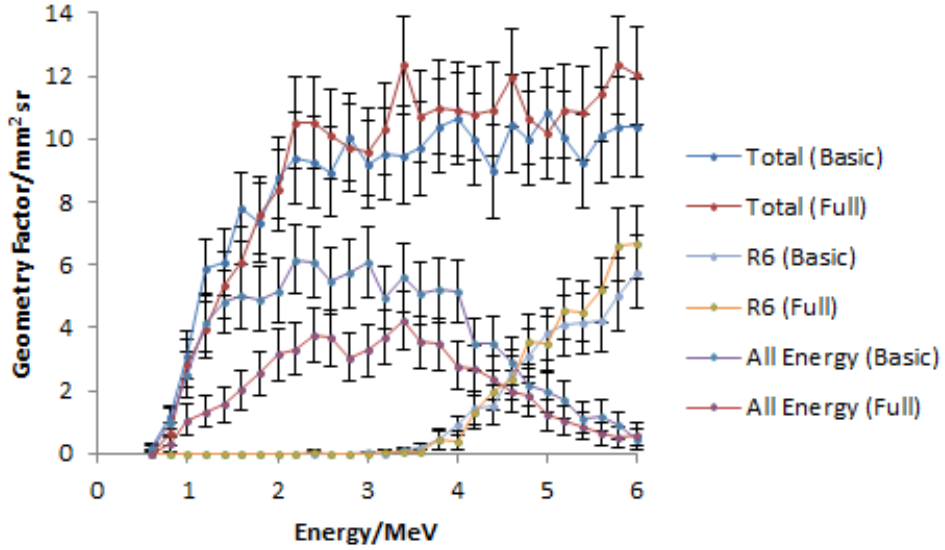

Figure 16: Comparison of geometry factors against energy for Total, All Energy and R6 events. Geometry factors for the basic model are in cool colors, while geometry factors for the full model are in warm colors.

factors for All Energy events in the full model.

5 Discussion

5.1 Incident Energy and Scattering

The degree of electron scattering by an atom is described by the differential cross-section of the atom, which decreases as the square proportionally to the inverse square of the incident energy of the electron. Thus, for a thin slab of material, the scattering by the material becomes smaller as the energy of the electron becomes larger. However, the situation changes if we instead have an infinitely thick slab of material. While the probability of scattering by each individual atom becomes smaller at higher energies, a high-energy electron will have a longer trajectory before it stops in the slab, and consequently will interact with more atoms. Assuming that the energy loss by the electron into the material is gradual, a high energy electron will eventually become a low energy electron at some point in the slab, only that it would have been scattered numerous times in its trajectory before it loses sufficient energy to reach that state. Thus we can see that in the case of an infinite slab of material, scattering increases with increasing incident energy.

These two competing effects can be clearly seen from both Figures 10 and 14. We first look at the curves for the Total events. At low incident energies, the geometry factor is small because electrons do not have sufficient energy to make it through H1i to reach H2, and the H2 coincidence criterion will not be satisfied. However, the greater scattering associated with lower energies also means that electrons with θ originally greater than the opening angle are more likely to be scattered inward to hit H2. This effectively broadens the $\theta = 0$ peak towards higher θ values (Figures 9 and 13), resulting in larger geometry factors due to the $\sin\theta$ dependence. Thus we see that as incident energy increases, the geometry factor for Total events increases rapidly initially after the minimum energy criterion is met, and then declines gradually as the peak in effective area slowly becomes narrower.

The geometry factor for combined All Energy + R6 events increases rapidly initially for the same reason that electrons require a minimum energy to reach H2. The geometry factor then peaks at 2.6 MeV before bottoming out at about 4 MeV and then increasing again. This is again a direct consequence of the two competing effects of incident energy on scattering. For lower energy electrons that stop in H2-H5, the detectors effectively act as an infinitely thick slab. Thus scattering increases with increasing incident energy, decreasing the geometry factor. However, after the minimum energy of 3.2 MeV, electrons can now completely pass through the HET without stopping, and the H2-H5 detectors become more and more like a thin slab as the electron trajectories become longer. This opposite effect of increasing the geometry factor gradually cancels out the first effect, eventually resulting in the geometry factor increasing at high incident energies. While this is beyond the scope of our study, we expect this rise in geometry factor to eventually plateau at very high electron energies. At these energies, electron trajectories are essentially straight with minimal scattering, and thus the geometry factor will be entirely due to the telescope geometry.

5.2 Effects of Non-Detecting Elements

Although we find the same qualitative features in the simulation results using both the basic and the full models, the presence of the non-detecting elements has in fact made it less straightforward to determine the incident energy distribution. The variability of the energy loss through the two Kapton windows results in a shifting and broadening of the diagonal ridge of All Energy events. We have seen that this effect makes it difficult to pick an appropriate buffer value to correctly identify electrons that stop in the detectors and to distinguish them from electrons that escape out the sides.

Scattering off the non-detecting elements also results in the higher geometry factors for the full model. As discussed earlier, electrons with high incident θ originally can be scattered back towards the telescope axis to create successful events. However, this increase in geometry factor is not favorable. A high-energy electron scattering off a non-detecting element and losing energy in the process gives a signal similar to a low-energy non-scattering electron. This results in broader response curves for particular incident energies.

6 Conclusion

We have developed a versatile simulation program using GEANT4 libraries, and investigated the electron response of the STEREO HET with two different models of the instrument. In a stark contrast to protons and heavier ions, we found that electron scattering has significant effects on the geometry factor of the instrument, and the dependence of this scattering on the incident energy of the electron gives rise to broader response curves and more complex features in the curves. The non-detecting elements of the HET provide even more objects to scatter the electrons. Despite these difficulties, it is possible to calibrate the instrument in order to quantitatively determine the distribution of incident energies, and we have provided such a theoretical calibration based on our simulation data.

The simulations that we have conducted, while definitely not a comprehensive investigation of the various aspects of the design of the HET, offer some insights into the basic design principles for particle instruments. The significant variability introduced by merely two Kapton films highlight the dangers of having excessive non-detecting elements in the instrument. A minimalist principle should drive the design of any similar instrument, and this principle is manifested in the cavernous design of the HET. Of course, were there no other design constrants, the most minimal design would be that of the basic model we have used, with the detectors completely exposed to a particle beam. However, not only do we have micrometeroids which can easily damage any exposed fragile silicon disks, the silicon disks are also sensitive to sunlight. Thus, some kind of protection is always necessary, and a balance has to be sought to provide this protection through good housing design without causing too much electron scattering. In addition, we have an omnidirectional source in space. The omnidirectional source in the space environment means that there will always be a background from electrons with sufficiently high energy to penetrate the housing. The problems of scattering by non-detecting elements can be mitigated by using active detecting elements with the appropriate anti-coincidence criteria to remove any event that are scattered off these elements. In this case, another balance has to be sought. Statistically, overly constraining the particle trajectories can result in excessively small count rates and thus relatively high uncertainties. Practically, additional detectors also translate into higher costs in both the actual detectors and the supporting electronics and power to manage the additional detectors and the higher count rates that result. Ultimately, all these considerations have to be taken into account in order to strick a delicate balance within the tight constraints of spacecraft instrument design.

Acknowledgments

This research is supported by the Homer J. Stewart endowment through the Summer Undergraduate Research Fellowship program of the California Institute of Technology.

References

[1] D. V. Reames. Particle Acceleration at the Sun and in the Heliosphere. *Space Science Reviews*, 90(3): 413–491, 1999.

[2] F. Guo and J. Giacalone. The Acceleration of Electrons at Perpendicular Shocks and its Implication for Solar Energetic Particle Events. In *Space Weather: The Space Radiation Environment*, pages 93–99, 2012.

[3] NASA. Solar Terrestial Probes Program (STP). http://stp.gsfc.nasa.gov/program_details.html. Accessed: 02/16/2013.

[4] D. Rust, J. Davila, V. Bothmer, L. Culhane, R. Fisher, J. Gosling, L. Guhathakurta, H. Hudson, M. Kaiser, J. Klimchuk, P. Liewer, R. Mewaldt, M. Neugebauer, V. Pizzo, D. Socker, K. Strong, G. Withbroe, and J. Watzin. *The Sun and Heliosphere in three dimensions: Report of the NASA Science Definition Team for the STEREO mission.* Johns Hopkins University Applied Physics Laboratory, 1997.

[5] T. T. von Rosenvinge, D. V. Reames, R. Baker, J. Hawk, J. T. Nolan, L. Ryan, S. Shuman, K. A. Wortman, R. A. Mewaldt, A. C. Cummings, W. R. Cook, A. W. Labrador, R. A. Leske, and M. E. Wiedenbeck. The High Energy Telescope for STEREO. *Space Science Reviews*, 136(1):391–435, 2008.

[6] D. K. Haggerty and E. C Roelof. Probing SEP Acceleration Processes With Near-relativistic Electrons. In *AIP Conference Proceedings*, volume 1183, page 3, 2009.

[7] E. W. Cliver. A Revised Classification Scheme for Solar Energetic Particle Events. *Central European Astrophysical Bulletin*, 33:253–270, 2009.

[8] F S Goulding and B G Harvey. Identification of nuclear particles. *Annual Review of Nuclear Science*, 25(1):167–240, 1975. doi: 10.1146/annurev.ns.25.120175.001123.

[9] J. D. Sullivan. Geometric factor and directional response of single and multi-element particle telescopes. *Nuclear Instruments and Methods*, 95(1):5–11, 1971.

[10] S. Agostinelli, J. Allison, K. Amako, J. Apostolakis, H. Araujo, P. Arce, M. Asai, D. Axen, S. Banerjee, G. Barrand, F. Behner, L. Bellagamba, J. Boudreau, L. Broglia, A. Brunengo, H. Burkhardt, S. Chauvie, J. Chuma, R. Chytracek, G. Cooperman, G. Cosmo, P. Degtyarenko, A. Dell'Acqua, G. Depaola, D. Dietrich, R. Enami, A. Feliciello, C. Ferguson, H. Fesefeldt, G. Folger, F. Foppiano, A. Forti, S. Garelli, S. Giani, R. Giannitrapani, D. Gibin, J.J. Gomez Cadenas, I. Gonzalez, G. Gracia Abril, G. Greeniaus, W. Greiner, V. Grichine, A. Grossheim, S. Guatelli, P. Gumplinger, R. Hamatsu, K. Hashimoto, H. Hasui, A. Heikkinen, A. Howard, V. Ivanchenko, A. Johnson, F.W. Jones, J. Kallenbach, N. Kanaya, M. Kawabata, Y. Kawabata, M. Kawaguti, S. Kelner, P. Kent, A. Kimura, T. Kodama, R. Kokoulin, M. Kossov, H. Kurashige, E. Lamanna, T. Lampen, V. Lara, V. Lefebure, F. Lei, M. Liendl, W. Lockman, F. Longo, S. Magni, M. Maire, E. Medernach, K. Minamimoto, P. Mora de Freitas, Y. Morita, K. Murakami, M. Nagamatu, R. Nartallo, P. Nieminen, T. Nishimura, K. Ohtsubo, M. Okamura, S. O'Neale, Y. Oohata, K. Paech, J. Perl, A. Pfeiffer, M.G. Pia, F. Ranjard, A. Rybin, S. Sadilov, E. Di Salvo, G. Santin, T. Sasaki, N. Savvas, Y. Sawada, S. Scherer, S. Sei, V. Sirotenko, D. Smith, N. Starkov, H. Stoecker, J. Sulkimo, M. Takahata, S. Tanaka, E. Tcherniaev, E. Safai Tehrani, M. Tropeano, P. Truscott, H. Uno, L. Urban, P. Urban, M. Verderi, A. Walkden, W. Wander, H. Weber, J.P. Wellisch, T. Wenaus, D.C. Williams, D. Wright, T. Yamada, H. Yoshida, and D. Zschiesche. Geant4: A simulation toolkit. *Nuclear Instruments and Methods in Physics Research Section A: Accelerators, Spectrometers, Detectors and Associated Equipment*, 506(3):250–303, 2003. ISSN 0168-9002.

[11] Magdalena Constantin, Dragos E Constantin, Paul J Keall, Anisha Narula, Michelle Svatos, and Joseph Perl. Linking computer-aided design (CAD) to geant4-based monte carlo simulations for precise implementation of complex treatment head geometries. *Physics in Medicine and Biology*, 55(8):N211, 2010.

Appendix I: Computation of Effective Areas and Geometry Factors

We define the probability $P(\theta, E)$ of having a successful event (i.e. satisfying one of the various coincidence criteria) at a particular incident polar angle θ and energy E:

$$P(\theta, E) = \frac{\text{Successful events}}{\text{Total events}}$$

where, in our simulations, the total number of events is a constant 5000. The azimuthal symmetry of our HET model implies the ϕ-independence of P.

The effective area A is calculated via

$$A(\theta, E) = P(\theta, E) \times (\text{Area of aperture})$$

where the area of the aperture is $\pi(18\text{ mm})^2 = 10\text{ cm}^2$. Uncertainties in the effective area are calculated assuming the binomial distribution:

$$Var(A) = \frac{P(1-P)}{\text{Total events}}(\text{Area of aperture})^2, \quad \Delta A = \sqrt{Var(A)}$$

The geometry factor G is calculated with

$$G(E) = 2\pi \int_0^{\pi/2} A(\theta, E) \sin\theta d\theta$$

by fitting a cubic spline for $A(\theta, E)$ at each value of E and then computing the integral using adaptive Gauss-Kronrod quadrature in MATLAB. The uncertainty is calculated in a similar way using

$$Var(G) = 2\pi \int_0^{\pi/2} Var(A) \sin\theta d\theta, \quad \Delta G = \sqrt{Var(G)}$$

Appendix II: Geometry Factors

A. Basic Model

Total Events

Detected Energy/MeV	Incident Energy/MeV													
	0.6	0.8	1.0	1.2	1.4	1.6	1.8	2.0	2.2	2.4	2.6	2.8	3.0	3.2
0-<0.2	0.000	0.000	0.000	0.000	0.000	0.000	0.000	0.000	0.000	0.000	0.000	0.000	0.000	0.000
0.2-<0.4	0.029	0.000	0.001	0.029	0.000	0.010	0.064	0.000	0.000	0.000	0.000	0.113	0.000	0.019
0.4-<0.6	0.106	0.048	0.039	0.349	0.010	0.000	0.002	0.000	0.010	0.096	0.000	0.039	0.000	0.001
0.6-<0.8	0.029	1.074	0.507	0.201	0.180	0.301	0.297	0.011	0.019	0.001	0.039	0.056	0.001	0.029
0.8-<1.0	0.000	0.038	2.536	0.477	0.521	0.436	0.340	0.263	0.233	0.128	0.197	0.086	0.039	0.057
1.0-<1.2	0.000	0.000	0.029	4.546	0.157	0.786	0.114	0.240	0.343	0.264	0.224	0.181	0.361	0.039
1.2-<1.4	0.000	0.000	0.000	0.292	4.128	0.431	0.474	0.525	0.378	0.455	0.200	0.117	0.095	0.258
1.4-<1.6	0.000	0.000	0.000	0.000	1.070	4.812	0.527	0.602	0.364	0.424	0.153	0.245	0.150	0.408
1.6-<1.8	0.000	0.000	0.000	0.000	0.000	1.047	4.321	0.531	0.213	0.277	0.239	0.297	0.197	0.146
1.8-<2.0	0.000	0.000	0.000	0.000	0.000	0.000	1.210	5.440	0.643	0.216	0.360	0.622	0.098	0.378
2.0-<2.2	0.000	0.000	0.000	0.000	0.000	0.000	0.000	1.161	5.031	0.511	0.451	0.525	0.152	0.491
2.2-<2.4	0.000	0.000	0.000	0.000	0.000	0.000	0.000	0.000	2.165	4.701	0.439	0.287	0.115	0.271
2.4-<2.6	0.000	0.000	0.000	0.000	0.000	0.000	0.000	0.000	0.000	2.181	5.233	0.477	0.332	0.350
2.6-<2.8	0.000	0.000	0.000	0.000	0.000	0.000	0.000	0.000	0.000	0.000	1.413	5.075	0.607	0.627
2.8-<3.0	0.000	0.000	0.000	0.000	0.000	0.000	0.000	0.000	0.000	0.000	0.000	1.918	4.435	0.507
3.0-<3.2	0.000	0.000	0.000	0.000	0.000	0.000	0.000	0.000	0.000	0.000	0.000	0.000	2.634	3.987
3.2-<3.4	0.000	0.000	0.000	0.000	0.000	0.000	0.000	0.000	0.000	0.000	0.000	0.000	0.000	1.974
3.4-<3.6	0.000	0.000	0.000	0.000	0.000	0.000	0.000	0.000	0.000	0.000	0.000	0.000	0.000	0.000
3.6-<3.8	0.000	0.000	0.000	0.000	0.000	0.000	0.000	0.000	0.000	0.000	0.000	0.000	0.000	0.000
3.8<-3.0	0.000	0.000	0.000	0.000	0.000	0.000	0.000	0.000	0.000	0.000	0.000	0.000	0.000	0.000
4.0-<4.2	0.000	0.000	0.000	0.000	0.000	0.000	0.000	0.000	0.000	0.000	0.000	0.000	0.000	0.000
4.2-<4.4	0.000	0.000	0.000	0.000	0.000	0.000	0.000	0.000	0.000	0.000	0.000	0.000	0.000	0.000
4.4-<4.6	0.000	0.000	0.000	0.000	0.000	0.000	0.000	0.000	0.000	0.000	0.000	0.000	0.000	0.000
4.6-<4.8	0.000	0.000	0.000	0.000	0.000	0.000	0.000	0.000	0.000	0.000	0.000	0.000	0.000	0.000
4.8-<5.0	0.000	0.000	0.000	0.000	0.000	0.000	0.000	0.000	0.000	0.000	0.000	0.000	0.000	0.000
4.0-<5.2	0.000	0.000	0.000	0.000	0.000	0.000	0.000	0.000	0.000	0.000	0.000	0.000	0.000	0.000
5.2-<5.4	0.000	0.000	0.000	0.000	0.000	0.000	0.000	0.000	0.000	0.000	0.000	0.000	0.000	0.000

	5.4-<5.6	0.000	0.000	0.000	0.000	0.000	0.000	0.000	0.000	0.000	0.000	0.000	0.000	0.000	0.000
	5.6-<5.8	0.000	0.000	0.000	0.000	0.000	0.000	0.000	0.000	0.000	0.000	0.000	0.000	0.000	0.000
	5.8-<6.0	0.000	0.000	0.000	0.000	0.000	0.000	0.000	0.000	0.000	0.000	0.000	0.000	0.000	0.000

		Incident Energy/MeV													
		3.4	3.6	3.8	4.0	4.2	4.4	4.6	4.8	5.0	5.2	5.4	5.6	5.8	6.0
Detected Energy/MeV	0-<0.2	0.000	0.000	0.000	0.000	0.000	0.000	0.000	0.000	0.000	0.000	0.000	0.000	0.000	0.000
	0.2-<0.4	0.000	0.000	0.000	0.010	0.000	0.000	0.000	0.000	0.038	0.000	0.000	0.000	0.010	0.000
	0.4-<0.6	0.000	0.056	0.000	0.010	0.019	0.019	0.000	0.019	0.001	0.000	0.000	0.000	0.000	0.000
	0.6-<0.8	0.038	0.011	0.076	0.010	0.065	0.065	0.000	0.011	0.000	0.000	0.000	0.000	0.000	0.019
	0.8-<1.0	0.064	0.001	0.001	0.000	0.030	0.030	0.000	0.000	0.038	0.038	0.082	0.000	0.056	0.010
	1.0-<1.2	0.001	0.030	0.076	0.029	0.029	0.029	0.110	0.103	0.029	0.010	0.038	0.000	0.057	0.000
	1.2-<1.4	0.040	0.031	0.140	0.067	0.149	0.149	0.059	0.079	0.056	0.040	0.000	0.157	0.001	0.136
	1.4-<1.6	0.191	0.096	0.039	0.049	0.029	0.029	0.010	0.093	0.000	0.029	0.019	0.126	0.030	0.000
	1.6-<1.8	0.372	0.188	0.165	0.163	0.098	0.098	0.039	0.115	0.076	0.058	0.056	0.189	0.094	0.072
	1.8-<2.0	0.135	0.229	0.115	0.097	0.228	0.228	0.095	0.076	0.196	0.067	0.040	0.070	0.000	0.161
	2.0-<2.2	0.209	0.147	0.174	0.225	0.087	0.087	0.096	0.042	0.117	0.115	0.116	0.153	0.049	0.106
	2.2-<2.4	0.161	0.247	0.278	0.165	0.171	0.171	0.154	0.095	0.214	0.100	0.181	0.127	0.240	0.049
	2.4-<2.6	0.217	0.245	0.314	0.220	0.134	0.134	0.543	0.344	0.138	0.225	0.175	0.278	0.347	0.196
	2.6-<2.8	0.329	0.277	0.293	0.267	0.201	0.201	0.314	0.337	0.658	0.604	0.514	0.466	0.823	0.596
	2.8-<3.0	0.499	0.454	0.497	0.356	0.568	0.568	0.492	0.613	0.766	0.934	0.769	1.019	0.828	0.911
	3.0-<3.2	0.389	0.405	0.432	0.565	0.587	0.587	0.648	0.507	0.893	0.814	0.887	0.952	0.998	1.357
	3.2-<3.4	4.192	0.895	0.597	0.698	0.636	0.636	0.743	0.800	0.837	0.942	0.809	1.015	0.839	0.926
	3.4-<3.6	2.641	4.131	1.006	0.520	0.674	0.674	0.873	0.902	0.726	0.651	0.770	0.608	0.931	0.990
	3.6-<3.8	0.000	2.252	3.676	0.831	0.700	0.700	0.534	0.612	0.859	0.626	0.679	0.640	0.519	0.606
	3.8<-3.0	0.000	0.000	2.517	4.326	1.194	1.194	0.745	0.312	0.568	0.670	0.417	0.419	0.613	0.552
	4.0-<4.2	0.000	0.000	0.000	2.037	2.622	2.622	0.546	0.440	0.523	0.610	0.465	0.395	0.288	0.403
	4.2-<4.4	0.000	0.000	0.000	0.000	1.758	1.758	0.510	0.617	0.763	0.314	0.470	0.395	0.294	0.682
	4.4-<4.6	0.000	0.000	0.000	0.000	0.000	0.000	2.516	0.465	0.480	0.274	0.243	0.417	0.351	0.358
	4.6-<4.8	0.000	0.000	0.000	0.000	0.000	0.000	1.451	2.570	0.419	0.241	0.298	0.198	0.410	0.247
	4.8-<5.0	0.000	0.000	0.000	0.000	0.000	0.000	0.000	0.859	1.321	0.467	0.367	0.322	0.243	0.258
	4.0-<5.2	0.000	0.000	0.000	0.000	0.000	0.000	0.000	0.000	1.107	1.523	0.390	0.167	0.179	0.278
	5.2-<5.4	0.000	0.000	0.000	0.000	0.000	0.000	0.000	0.000	0.000	0.690	0.949	0.270	0.356	0.145
	5.4-<5.6	0.000	0.000	0.000	0.000	0.000	0.000	0.000	0.000	0.000	0.000	0.548	1.137	0.272	0.184

	5.6-<5.8	0.000	0.000	0.000	0.000	0.000	0.000	0.000	0.000	0.000	0.000	0.000	0.608	1.213	0.376
	5.8-<6.0	0.000	0.000	0.000	0.000	0.000	0.000	0.000	0.000	0.000	0.000	0.000	0.000	0.333	0.550

R2 Events

		Incident Energy/MeV													
		0.6	0.8	1.0	1.2	1.4	1.6	1.8	2.0	2.2	2.4	2.6	2.8	3.0	3.2
Detected Energy/MeV	0-<0.2	0.000	0.000	0.000	0.000	0.000	0.000	0.000	0.000	0.000	0.000	0.000	0.000	0.000	0.000
	0.2-<0.4	0.000	0.000	0.001	0.000	0.000	0.000	0.064	0.000	0.000	0.000	0.000	0.056	0.000	0.019
	0.4-<0.6	0.106	0.000	0.010	0.072	0.000	0.000	0.002	0.000	0.010	0.048	0.000	0.039	0.000	0.001
	0.6-<0.8	0.029	0.615	0.439	0.115	0.113	0.168	0.150	0.011	0.000	0.000	0.000	0.000	0.000	0.000
	0.8-<1.0	0.000	0.038	1.483	0.266	0.214	0.120	0.085	0.167	0.039	0.029	0.095	0.056	0.000	0.001
	1.0-<1.2	0.000	0.000	0.000	2.021	0.000	0.241	0.075	0.001	0.095	0.140	0.167	0.058	0.158	0.000
	1.2-<1.4	0.000	0.000	0.000	0.079	1.121	0.262	0.101	0.179	0.128	0.133	0.067	0.000	0.000	0.074
	1.4-<1.6	0.000	0.000	0.000	0.000	0.230	0.571	0.260	0.149	0.000	0.139	0.020	0.082	0.038	0.047
	1.6-<1.8	0.000	0.000	0.000	0.000	0.000	0.388	0.278	0.178	0.000	0.000	0.000	0.000	0.000	0.000
	1.8-<2.0	0.000	0.000	0.000	0.000	0.000	0.000	0.095	0.368	0.029	0.079	0.102	0.019	0.000	0.038
	2.0-<2.2	0.000	0.000	0.000	0.000	0.000	0.000	0.000	0.029	0.086	0.019	0.072	0.001	0.000	0.000
	2.2-<2.4	0.000	0.000	0.000	0.000	0.000	0.000	0.000	0.000	0.079	0.001	0.000	0.000	0.000	0.000
	2.4-<2.6	0.000	0.000	0.000	0.000	0.000	0.000	0.000	0.000	0.000	0.000	0.038	0.000	0.000	0.000
	2.6-<2.8	0.000	0.000	0.000	0.000	0.000	0.000	0.000	0.000	0.000	0.000	0.001	0.000	0.000	0.000
	2.8-<3.0	0.000	0.000	0.000	0.000	0.000	0.000	0.000	0.000	0.000	0.000	0.000	0.000	0.000	0.000
	3.0-<3.2	0.000	0.000	0.000	0.000	0.000	0.000	0.000	0.000	0.000	0.000	0.000	0.000	0.000	0.000
	3.2-<3.4	0.000	0.000	0.000	0.000	0.000	0.000	0.000	0.000	0.000	0.000	0.000	0.000	0.000	0.000
	3.4-<3.6	0.000	0.000	0.000	0.000	0.000	0.000	0.000	0.000	0.000	0.000	0.000	0.000	0.000	0.000
	3.6-<3.8	0.000	0.000	0.000	0.000	0.000	0.000	0.000	0.000	0.000	0.000	0.000	0.000	0.000	0.000
	3.8<-3.0	0.000	0.000	0.000	0.000	0.000	0.000	0.000	0.000	0.000	0.000	0.000	0.000	0.000	0.000
	4.0-<4.2	0.000	0.000	0.000	0.000	0.000	0.000	0.000	0.000	0.000	0.000	0.000	0.000	0.000	0.000
	4.2-<4.4	0.000	0.000	0.000	0.000	0.000	0.000	0.000	0.000	0.000	0.000	0.000	0.000	0.000	0.000
	4.4-<4.6	0.000	0.000	0.000	0.000	0.000	0.000	0.000	0.000	0.000	0.000	0.000	0.000	0.000	0.000
	4.6-<4.8	0.000	0.000	0.000	0.000	0.000	0.000	0.000	0.000	0.000	0.000	0.000	0.000	0.000	0.000
	4.8-<5.0	0.000	0.000	0.000	0.000	0.000	0.000	0.000	0.000	0.000	0.000	0.000	0.000	0.000	0.000
	4.0-<5.2	0.000	0.000	0.000	0.000	0.000	0.000	0.000	0.000	0.000	0.000	0.000	0.000	0.000	0.000
	5.2-<5.4	0.000	0.000	0.000	0.000	0.000	0.000	0.000	0.000	0.000	0.000	0.000	0.000	0.000	0.000

	5.4-<5.6	0.000	0.000	0.000	0.000	0.000	0.000	0.000	0.000	0.000	0.000	0.000	0.000	0.000	0.000
	5.6-<5.8	0.000	0.000	0.000	0.000	0.000	0.000	0.000	0.000	0.000	0.000	0.000	0.000	0.000	0.000
	5.8-<6.0	0.000	0.000	0.000	0.000	0.000	0.000	0.000	0.000	0.000	0.000	0.000	0.000	0.000	0.000

		Incident Energy/MeV													
		3.4	3.6	3.8	4.0	4.2	4.4	4.6	4.8	5.0	5.2	5.4	5.6	5.8	6.0
Detected Energy/MeV	0-<0.2	0.000	0.000	0.000	0.000	0.000	0.000	0.000	0.000	0.000	0.000	0.000	0.000	0.000	0.000
	0.2-<0.4	0.000	0.000	0.000	0.000	0.000	0.000	0.000	0.000	0.000	0.000	0.000	0.000	0.000	0.000
	0.4-<0.6	0.000	0.056	0.000	0.000	0.000	0.000	0.000	0.000	0.000	0.000	0.000	0.000	0.000	0.000
	0.6-<0.8	0.038	0.001	0.056	0.000	0.065	0.029	0.000	0.000	0.000	0.000	0.000	0.000	0.000	0.019
	0.8-<1.0	0.000	0.000	0.001	0.000	0.029	0.000	0.000	0.000	0.038	0.038	0.000	0.000	0.056	0.010
	1.0-<1.2	0.001	0.030	0.000	0.000	0.000	0.000	0.000	0.000	0.000	0.000	0.000	0.000	0.038	0.000
	1.2-<1.4	0.000	0.000	0.064	0.010	0.000	0.029	0.000	0.000	0.056	0.000	0.000	0.000	0.000	0.019
	1.4-<1.6	0.000	0.029	0.000	0.001	0.000	0.000	0.000	0.000	0.000	0.029	0.000	0.010	0.000	0.000
	1.6-<1.8	0.072	0.000	0.000	0.019	0.000	0.000	0.000	0.000	0.029	0.000	0.000	0.000	0.000	0.000
	1.8-<2.0	0.000	0.000	0.000	0.000	0.000	0.000	0.000	0.000	0.072	0.000	0.000	0.000	0.000	0.000
	2.0-<2.2	0.072	0.000	0.000	0.000	0.000	0.000	0.000	0.038	0.000	0.000	0.000	0.000	0.000	0.000
	2.2-<2.4	0.000	0.000	0.000	0.000	0.000	0.000	0.000	0.000	0.000	0.000	0.001	0.000	0.000	0.000
	2.4-<2.6	0.000	0.000	0.000	0.000	0.000	0.000	0.000	0.000	0.000	0.000	0.000	0.000	0.000	0.000
	2.6-<2.8	0.000	0.000	0.000	0.000	0.000	0.000	0.000	0.000	0.000	0.000	0.000	0.000	0.000	0.000
	2.8-<3.0	0.000	0.000	0.000	0.000	0.000	0.000	0.000	0.000	0.000	0.000	0.000	0.000	0.000	0.000
	3.0-<3.2	0.000	0.000	0.000	0.000	0.000	0.000	0.000	0.000	0.000	0.000	0.000	0.000	0.000	0.000
	3.2-<3.4	0.000	0.000	0.000	0.000	0.000	0.000	0.000	0.000	0.000	0.000	0.000	0.000	0.000	0.000
	3.4-<3.6	0.010	0.000	0.000	0.000	0.000	0.000	0.000	0.000	0.000	0.000	0.000	0.000	0.000	0.000
	3.6-<3.8	0.000	0.000	0.000	0.000	0.000	0.000	0.000	0.000	0.000	0.000	0.000	0.000	0.000	0.000
	3.8<-3.0	0.000	0.000	0.000	0.000	0.000	0.000	0.000	0.000	0.000	0.000	0.000	0.000	0.000	0.000
	4.0-<4.2	0.000	0.000	0.000	0.000	0.000	0.000	0.000	0.000	0.000	0.000	0.000	0.000	0.000	0.000
	4.2-<4.4	0.000	0.000	0.000	0.000	0.000	0.000	0.000	0.000	0.000	0.000	0.000	0.000	0.000	0.000
	4.4-<4.6	0.000	0.000	0.000	0.000	0.000	0.000	0.000	0.000	0.000	0.000	0.000	0.000	0.000	0.000
	4.6-<4.8	0.000	0.000	0.000	0.000	0.000	0.000	0.000	0.000	0.000	0.000	0.000	0.000	0.000	0.000
	4.8-<5.0	0.000	0.000	0.000	0.000	0.000	0.000	0.000	0.000	0.000	0.000	0.000	0.000	0.000	0.000
	4.0-<5.2	0.000	0.000	0.000	0.000	0.000	0.000	0.000	0.000	0.000	0.000	0.000	0.000	0.000	0.000
	5.2-<5.4	0.000	0.000	0.000	0.000	0.000	0.000	0.000	0.000	0.000	0.000	0.000	0.000	0.000	0.000
	5.4-<5.6	0.000	0.000	0.000	0.000	0.000	0.000	0.000	0.000	0.000	0.000	0.000	0.000	0.000	0.000

	5.6-<5.8	0.000	0.000	0.000	0.000	0.000	0.000	0.000	0.000	0.000	0.000	0.000	0.000	0.000	0.000
	5.8-<6.0	0.000	0.000	0.000	0.000	0.000	0.000	0.000	0.000	0.000	0.000	0.000	0.000	0.000	0.000

R3 Events

		Incident Energy/MeV													
		0.6	0.8	1.0	1.2	1.4	1.6	1.8	2.0	2.2	2.4	2.6	2.8	3.0	3.2
Detected Energy/MeV	0-<0.2	0.000	0.000	0.000	0.000	0.000	0.000	0.000	0.000	0.000	0.000	0.000	0.000	0.000	0.000
	0.2-<0.4	0.000	0.000	0.000	0.000	0.000	0.000	0.000	0.000	0.000	0.000	0.000	0.000	0.000	0.000
	0.4-<0.6	0.000	0.000	0.000	0.000	0.000	0.000	0.000	0.000	0.000	0.000	0.000	0.000	0.000	0.000
	0.6-<0.8	0.000	0.010	0.000	0.000	0.000	0.000	0.048	0.000	0.000	0.000	0.000	0.000	0.000	0.029
	0.8-<1.0	0.000	0.000	0.010	0.079	0.074	0.120	0.072	0.038	0.057	0.000	0.038	0.001	0.000	0.000
	1.0-<1.2	0.000	0.000	0.029	0.882	0.064	0.120	0.039	0.133	0.154	0.104	0.000	0.038	0.066	0.038
	1.2-<1.4	0.000	0.000	0.000	0.067	1.276	0.131	0.122	0.158	0.011	0.171	0.029	0.039	0.000	0.038
	1.4-<1.6	0.000	0.000	0.000	0.000	0.406	2.366	0.030	0.183	0.214	0.124	0.114	0.104	0.072	0.147
	1.6-<1.8	0.000	0.000	0.000	0.000	0.000	0.378	1.969	0.232	0.000	0.217	0.239	0.286	0.159	0.069
	1.8-<2.0	0.000	0.000	0.000	0.000	0.000	0.000	0.304	2.360	0.513	0.098	0.218	0.194	0.088	0.182
	2.0-<2.2	0.000	0.000	0.000	0.000	0.000	0.000	0.000	0.699	2.214	0.220	0.096	0.327	0.122	0.232
	2.2-<2.4	0.000	0.000	0.000	0.000	0.000	0.000	0.000	0.000	1.022	1.669	0.268	0.087	0.050	0.049
	2.4-<2.6	0.000	0.000	0.000	0.000	0.000	0.000	0.000	0.000	0.000	1.071	1.292	0.178	0.160	0.218
	2.6-<2.8	0.000	0.000	0.000	0.000	0.000	0.000	0.000	0.000	0.000	0.000	0.564	0.950	0.181	0.095
	2.8-<3.0	0.000	0.000	0.000	0.000	0.000	0.000	0.000	0.000	0.000	0.000	0.000	0.508	0.998	0.029
	3.0-<3.2	0.000	0.000	0.000	0.000	0.000	0.000	0.000	0.000	0.000	0.000	0.000	0.000	0.854	0.629
	3.2-<3.4	0.000	0.000	0.000	0.000	0.000	0.000	0.000	0.000	0.000	0.000	0.000	0.000	0.000	0.370
	3.4-<3.6	0.000	0.000	0.000	0.000	0.000	0.000	0.000	0.000	0.000	0.000	0.000	0.000	0.000	0.000
	3.6-<3.8	0.000	0.000	0.000	0.000	0.000	0.000	0.000	0.000	0.000	0.000	0.000	0.000	0.000	0.000
	3.8<-3.0	0.000	0.000	0.000	0.000	0.000	0.000	0.000	0.000	0.000	0.000	0.000	0.000	0.000	0.000
	4.0-<4.2	0.000	0.000	0.000	0.000	0.000	0.000	0.000	0.000	0.000	0.000	0.000	0.000	0.000	0.000
	4.2-<4.4	0.000	0.000	0.000	0.000	0.000	0.000	0.000	0.000	0.000	0.000	0.000	0.000	0.000	0.000
	4.4-<4.6	0.000	0.000	0.000	0.000	0.000	0.000	0.000	0.000	0.000	0.000	0.000	0.000	0.000	0.000
	4.6-<4.8	0.000	0.000	0.000	0.000	0.000	0.000	0.000	0.000	0.000	0.000	0.000	0.000	0.000	0.000
	4.8-<5.0	0.000	0.000	0.000	0.000	0.000	0.000	0.000	0.000	0.000	0.000	0.000	0.000	0.000	0.000
	4.0-<5.2	0.000	0.000	0.000	0.000	0.000	0.000	0.000	0.000	0.000	0.000	0.000	0.000	0.000	0.000
	5.2-<5.4	0.000	0.000	0.000	0.000	0.000	0.000	0.000	0.000	0.000	0.000	0.000	0.000	0.000	0.000

	5.4-<5.6	0.000	0.000	0.000	0.000	0.000	0.000	0.000	0.000	0.000	0.000	0.000	0.000	0.000	0.000
	5.6-<5.8	0.000	0.000	0.000	0.000	0.000	0.000	0.000	0.000	0.000	0.000	0.000	0.000	0.000	0.000
	5.8-<6.0	0.000	0.000	0.000	0.000	0.000	0.000	0.000	0.000	0.000	0.000	0.000	0.000	0.000	0.000

		Incident Energy/MeV													
		3.4	3.6	3.8	4.0	4.2	4.4	4.6	4.8	5.0	5.2	5.4	5.6	5.8	6.0
Detected Energy/MeV	0-<0.2	0.000	0.000	0.000	0.000	0.000	0.000	0.000	0.000	0.000	0.000	0.000	0.000	0.000	0.000
	0.2-<0.4	0.000	0.000	0.000	0.000	0.000	0.000	0.000	0.000	0.000	0.000	0.000	0.000	0.000	0.000
	0.4-<0.6	0.000	0.000	0.000	0.000	0.000	0.000	0.000	0.000	0.000	0.000	0.000	0.000	0.000	0.000
	0.6-<0.8	0.000	0.000	0.001	0.000	0.000	0.000	0.000	0.000	0.000	0.000	0.000	0.000	0.000	0.000
	0.8-<1.0	0.064	0.000	0.000	0.000	0.001	0.000	0.000	0.000	0.000	0.000	0.000	0.000	0.000	0.000
	1.0-<1.2	0.001	0.000	0.000	0.000	0.029	0.019	0.038	0.047	0.029	0.000	0.000	0.000	0.000	0.000
	1.2-<1.4	0.030	0.002	0.076	0.001	0.072	0.000	0.000	0.000	0.000	0.029	0.000	0.000	0.001	0.038
	1.4-<1.6	0.143	0.000	0.039	0.048	0.010	0.000	0.000	0.064	0.000	0.000	0.000	0.019	0.030	0.000
	1.6-<1.8	0.213	0.077	0.049	0.001	0.001	0.000	0.000	0.048	0.000	0.020	0.000	0.141	0.000	0.072
	1.8-<2.0	0.029	0.075	0.039	0.049	0.077	0.010	0.000	0.000	0.047	0.019	0.000	0.001	0.000	0.058
	2.0-<2.2	0.137	0.108	0.068	0.078	0.029	0.019	0.020	0.001	0.058	0.066	0.029	0.097	0.000	0.001
	2.2-<2.4	0.120	0.086	0.124	0.049	0.049	0.096	0.000	0.000	0.038	0.000	0.056	0.000	0.057	0.000
	2.4-<2.6	0.048	0.048	0.255	0.085	0.010	0.001	0.076	0.116	0.000	0.000	0.019	0.029	0.019	0.057
	2.6-<2.8	0.196	0.162	0.075	0.010	0.001	0.011	0.000	0.076	0.000	0.038	0.000	0.019	0.029	0.001
	2.8-<3.0	0.210	0.102	0.087	0.069	0.108	0.029	0.039	0.000	0.000	0.019	0.019	0.000	0.000	0.000
	3.0-<3.2	0.095	0.085	0.049	0.020	0.029	0.020	0.019	0.000	0.029	0.038	0.094	0.010	0.000	0.000
	3.2-<3.4	0.611	0.067	0.010	0.030	0.048	0.029	0.038	0.000	0.010	0.038	0.000	0.000	0.000	0.000
	3.4-<3.6	0.323	0.378	0.039	0.019	0.077	0.000	0.083	0.030	0.000	0.010	0.000	0.000	0.020	0.000
	3.6-<3.8	0.000	0.224	0.105	0.111	0.029	0.000	0.000	0.000	0.000	0.019	0.010	0.000	0.001	0.000
	3.8<-3.0	0.000	0.000	0.253	0.080	0.000	0.000	0.000	0.001	0.038	0.000	0.000	0.000	0.000	0.000
	4.0-<4.2	0.000	0.000	0.000	0.447	0.059	0.000	0.010	0.000	0.000	0.000	0.000	0.000	0.000	0.000
	4.2-<4.4	0.000	0.000	0.000	0.000	0.000	0.031	0.047	0.000	0.019	0.001	0.038	0.084	0.000	0.000
	4.4-<4.6	0.000	0.000	0.000	0.000	0.000	0.095	0.115	0.000	0.010	0.000	0.019	0.000	0.000	0.000
	4.6-<4.8	0.000	0.000	0.000	0.000	0.000	0.000	0.039	0.082	0.000	0.019	0.000	0.010	0.000	0.038
	4.8-<5.0	0.000	0.000	0.000	0.000	0.000	0.000	0.000	0.039	0.000	0.029	0.000	0.000	0.000	0.000
	4.0-<5.2	0.000	0.000	0.000	0.000	0.000	0.000	0.000	0.000	0.000	0.000	0.000	0.000	0.038	0.000
	5.2-<5.4	0.000	0.000	0.000	0.000	0.000	0.000	0.000	0.000	0.000	0.000	0.000	0.000	0.000	0.000
	5.4-<5.6	0.000	0.000	0.000	0.000	0.000	0.000	0.000	0.000	0.000	0.000	0.000	0.001	0.000	0.000

	5.6-<5.8	0.000	0.000	0.000	0.000	0.000	0.000	0.000	0.000	0.000	0.000	0.000	0.000	0.001	0.000
	5.8-<6.0	0.000	0.000	0.000	0.000	0.000	0.000	0.000	0.000	0.000	0.000	0.000	0.000	0.000	0.000

R4 Events

		Incident Energy/MeV													
		0.6	0.8	1.0	1.2	1.4	1.6	1.8	2.0	2.2	2.4	2.6	2.8	3.0	3.2
Detected Energy/MeV	0-<0.2	0.000	0.000	0.000	0.000	0.000	0.000	0.000	0.000	0.000	0.000	0.000	0.000	0.000	0.000
	0.2-<0.4	0.000	0.000	0.000	0.000	0.000	0.000	0.000	0.000	0.000	0.000	0.000	0.000	0.000	0.000
	0.4-<0.6	0.000	0.000	0.000	0.000	0.000	0.000	0.000	0.000	0.000	0.000	0.000	0.000	0.000	0.000
	0.6-<0.8	0.000	0.000	0.000	0.000	0.000	0.000	0.000	0.000	0.000	0.000	0.000	0.000	0.000	0.000
	0.8-<1.0	0.000	0.000	0.000	0.000	0.000	0.000	0.000	0.000	0.000	0.000	0.000	0.000	0.000	0.000
	1.0-<1.2	0.000	0.000	0.000	0.000	0.000	0.000	0.000	0.000	0.000	0.000	0.000	0.000	0.000	0.000
	1.2-<1.4	0.000	0.000	0.000	0.000	0.000	0.000	0.000	0.000	0.000	0.000	0.000	0.000	0.000	0.000
	1.4-<1.6	0.000	0.000	0.000	0.000	0.064	0.000	0.000	0.000	0.000	0.000	0.000	0.000	0.000	0.000
	1.6-<1.8	0.000	0.000	0.000	0.000	0.000	0.000	0.066	0.000	0.000	0.010	0.000	0.000	0.000	0.001
	1.8-<2.0	0.000	0.000	0.000	0.000	0.000	0.000	0.001	0.308	0.000	0.000	0.000	0.000	0.000	0.000
	2.0-<2.2	0.000	0.000	0.000	0.000	0.000	0.000	0.000	0.029	0.994	0.168	0.074	0.001	0.010	0.105
	2.2-<2.4	0.000	0.000	0.000	0.000	0.000	0.000	0.000	0.000	0.059	0.716	0.083	0.056	0.064	0.086
	2.4-<2.6	0.000	0.000	0.000	0.000	0.000	0.000	0.000	0.000	0.000	0.281	0.908	0.096	0.078	0.038
	2.6-<2.8	0.000	0.000	0.000	0.000	0.000	0.000	0.000	0.000	0.000	0.000	0.270	1.814	0.276	0.178
	2.8-<3.0	0.000	0.000	0.000	0.000	0.000	0.000	0.000	0.000	0.000	0.000	0.000	0.586	1.495	0.143
	3.0-<3.2	0.000	0.000	0.000	0.000	0.000	0.000	0.000	0.000	0.000	0.000	0.000	0.000	0.863	1.298
	3.2-<3.4	0.000	0.000	0.000	0.000	0.000	0.000	0.000	0.000	0.000	0.000	0.000	0.000	0.000	0.696
	3.4-<3.6	0.000	0.000	0.000	0.000	0.000	0.000	0.000	0.000	0.000	0.000	0.000	0.000	0.000	0.000
	3.6-<3.8	0.000	0.000	0.000	0.000	0.000	0.000	0.000	0.000	0.000	0.000	0.000	0.000	0.000	0.000
	3.8<-3.0	0.000	0.000	0.000	0.000	0.000	0.000	0.000	0.000	0.000	0.000	0.000	0.000	0.000	0.000
	4.0-<4.2	0.000	0.000	0.000	0.000	0.000	0.000	0.000	0.000	0.000	0.000	0.000	0.000	0.000	0.000
	4.2-<4.4	0.000	0.000	0.000	0.000	0.000	0.000	0.000	0.000	0.000	0.000	0.000	0.000	0.000	0.000
	4.4-<4.6	0.000	0.000	0.000	0.000	0.000	0.000	0.000	0.000	0.000	0.000	0.000	0.000	0.000	0.000
	4.6-<4.8	0.000	0.000	0.000	0.000	0.000	0.000	0.000	0.000	0.000	0.000	0.000	0.000	0.000	0.000
	4.8-<5.0	0.000	0.000	0.000	0.000	0.000	0.000	0.000	0.000	0.000	0.000	0.000	0.000	0.000	0.000
	4.0-<5.2	0.000	0.000	0.000	0.000	0.000	0.000	0.000	0.000	0.000	0.000	0.000	0.000	0.000	0.000
	5.2-<5.4	0.000	0.000	0.000	0.000	0.000	0.000	0.000	0.000	0.000	0.000	0.000	0.000	0.000	0.000

	5.4-<5.6	0.000	0.000	0.000	0.000	0.000	0.000	0.000	0.000	0.000	0.000	0.000	0.000	0.000	0.000
	5.6-<5.8	0.000	0.000	0.000	0.000	0.000	0.000	0.000	0.000	0.000	0.000	0.000	0.000	0.000	0.000
	5.8-<6.0	0.000	0.000	0.000	0.000	0.000	0.000	0.000	0.000	0.000	0.000	0.000	0.000	0.000	0.000

		Incident Energy/MeV													
		3.4	3.6	3.8	4.0	4.2	4.4	4.6	4.8	5.0	5.2	5.4	5.6	5.8	6.0
Detected Energy/MeV	0-<0.2	0.000	0.000	0.000	0.000	0.000	0.000	0.000	0.000	0.000	0.000	0.000	0.000	0.000	0.000
	0.2-<0.4	0.000	0.000	0.000	0.000	0.000	0.000	0.000	0.000	0.000	0.000	0.000	0.000	0.000	0.000
	0.4-<0.6	0.000	0.000	0.000	0.000	0.000	0.000	0.000	0.000	0.000	0.000	0.000	0.000	0.000	0.000
	0.6-<0.8	0.000	0.000	0.000	0.000	0.000	0.000	0.000	0.000	0.000	0.000	0.000	0.000	0.000	0.000
	0.8-<1.0	0.000	0.000	0.000	0.000	0.000	0.000	0.000	0.000	0.000	0.000	0.000	0.000	0.000	0.000
	1.0-<1.2	0.000	0.000	0.000	0.000	0.000	0.000	0.000	0.000	0.000	0.000	0.000	0.000	0.000	0.000
	1.2-<1.4	0.000	0.000	0.000	0.000	0.000	0.000	0.000	0.000	0.000	0.000	0.000	0.000	0.000	0.000
	1.4-<1.6	0.000	0.038	0.000	0.000	0.000	0.000	0.000	0.000	0.000	0.000	0.000	0.000	0.000	0.000
	1.6-<1.8	0.029	0.064	0.000	0.001	0.001	0.000	0.000	0.019	0.047	0.000	0.000	0.000	0.000	0.000
	1.8-<2.0	0.000	0.048	0.019	0.010	0.038	0.038	0.057	0.019	0.047	0.019	0.001	0.029	0.000	0.001
	2.0-<2.2	0.000	0.010	0.000	0.117	0.038	0.038	0.076	0.003	0.020	0.019	0.087	0.056	0.029	0.057
	2.2-<2.4	0.030	0.086	0.067	0.020	0.057	0.030	0.040	0.047	0.102	0.079	0.001	0.059	0.125	0.001
	2.4-<2.6	0.139	0.158	0.019	0.001	0.039	0.040	0.131	0.129	0.030	0.067	0.095	0.049	0.058	0.020
	2.6-<2.8	0.058	0.000	0.133	0.064	0.057	0.069	0.059	0.077	0.133	0.125	0.076	0.106	0.000	0.060
	2.8-<3.0	0.087	0.185	0.226	0.134	0.125	0.161	0.105	0.105	0.104	0.020	0.068	0.123	0.000	0.050
	3.0-<3.2	0.086	0.174	0.068	0.188	0.168	0.140	0.058	0.021	0.115	0.047	0.039	0.089	0.056	0.096
	3.2-<3.4	1.030	0.339	0.114	0.160	0.058	0.058	0.058	0.200	0.135	0.020	0.030	0.146	0.039	0.039
	3.4-<3.6	0.790	1.218	0.325	0.172	0.134	0.039	0.135	0.094	0.123	0.048	0.019	0.049	0.115	0.056
	3.6-<3.8	0.000	0.763	1.256	0.021	0.030	0.098	0.059	0.121	0.106	0.072	0.049	0.067	0.067	0.048
	3.8<-3.0	0.000	0.000	0.617	0.741	0.350	0.174	0.030	0.022	0.167	0.048	0.001	0.116	0.019	0.040
	4.0-<4.2	0.000	0.000	0.000	0.525	0.662	0.172	0.078	0.000	0.020	0.060	0.039	0.056	0.030	0.000
	4.2-<4.4	0.000	0.000	0.000	0.000	0.469	0.692	0.049	0.088	0.108	0.020	0.029	0.000	0.001	0.101
	4.4-<4.6	0.000	0.000	0.000	0.000	0.000	0.572	0.664	0.029	0.104	0.001	0.000	0.040	0.039	0.000
	4.6-<4.8	0.000	0.000	0.000	0.000	0.000	0.000	0.236	0.379	0.106	0.094	0.048	0.020	0.001	0.000
	4.8-<5.0	0.000	0.000	0.000	0.000	0.000	0.000	0.000	0.189	0.395	0.057	0.029	0.011	0.020	0.049
	4.0-<5.2	0.000	0.000	0.000	0.000	0.000	0.000	0.000	0.000	0.149	0.308	0.011	0.058	0.000	0.047
	5.2-<5.4	0.000	0.000	0.000	0.000	0.000	0.000	0.000	0.000	0.000	0.108	0.147	0.057	0.086	0.019
	5.4-<5.6	0.000	0.000	0.000	0.000	0.000	0.000	0.000	0.000	0.000	0.000	0.116	0.173	0.001	0.000

	5.6-<5.8	0.000	0.000	0.000	0.000	0.000	0.000	0.000	0.000	0.000	0.000	0.000	0.096	0.156	0.010
	5.8-<6.0	0.000	0.000	0.000	0.000	0.000	0.000	0.000	0.000	0.000	0.000	0.000	0.000	0.011	0.040

R5 Events

		Incident Energy/MeV													
		0.6	0.8	1.0	1.2	1.4	1.6	1.8	2.0	2.2	2.4	2.6	2.8	3.0	3.2
Detected Energy/MeV	0-<0.2	0.000	0.000	0.000	0.000	0.000	0.000	0.000	0.000	0.000	0.000	0.000	0.000	0.000	0.000
	0.2-<0.4	0.000	0.000	0.000	0.000	0.000	0.000	0.000	0.000	0.000	0.000	0.000	0.000	0.000	0.000
	0.4-<0.6	0.000	0.000	0.000	0.000	0.000	0.000	0.000	0.000	0.000	0.000	0.000	0.000	0.000	0.000
	0.6-<0.8	0.000	0.000	0.000	0.000	0.000	0.000	0.000	0.000	0.000	0.000	0.000	0.000	0.000	0.000
	0.8-<1.0	0.000	0.000	0.000	0.000	0.000	0.000	0.000	0.000	0.000	0.000	0.000	0.000	0.000	0.000
	1.0-<1.2	0.000	0.000	0.000	0.000	0.000	0.000	0.000	0.000	0.000	0.000	0.000	0.000	0.000	0.000
	1.2-<1.4	0.000	0.000	0.000	0.000	0.000	0.000	0.000	0.000	0.000	0.000	0.000	0.000	0.000	0.000
	1.4-<1.6	0.000	0.000	0.000	0.000	0.000	0.000	0.000	0.000	0.000	0.000	0.000	0.000	0.000	0.000
	1.6-<1.8	0.000	0.000	0.000	0.000	0.000	0.000	0.000	0.000	0.000	0.000	0.000	0.000	0.000	0.000
	1.8-<2.0	0.000	0.000	0.000	0.000	0.000	0.000	0.000	0.000	0.000	0.000	0.000	0.000	0.000	0.000
	2.0-<2.2	0.000	0.000	0.000	0.000	0.000	0.000	0.000	0.000	0.000	0.000	0.000	0.000	0.000	0.000
	2.2-<2.4	0.000	0.000	0.000	0.000	0.000	0.000	0.000	0.000	0.038	0.000	0.000	0.001	0.000	0.000
	2.4-<2.6	0.000	0.000	0.000	0.000	0.000	0.000	0.000	0.000	0.000	0.000	0.122	0.000	0.000	0.064
	2.6-<2.8	0.000	0.000	0.000	0.000	0.000	0.000	0.000	0.000	0.000	0.000	0.000	0.151	0.000	0.010
	2.8-<3.0	0.000	0.000	0.000	0.000	0.000	0.000	0.000	0.000	0.000	0.000	0.000	0.065	0.369	0.011
	3.0-<3.2	0.000	0.000	0.000	0.000	0.000	0.000	0.000	0.000	0.000	0.000	0.000	0.000	0.049	0.223
	3.2-<3.4	0.000	0.000	0.000	0.000	0.000	0.000	0.000	0.000	0.000	0.000	0.000	0.000	0.000	0.218
	3.4-<3.6	0.000	0.000	0.000	0.000	0.000	0.000	0.000	0.000	0.000	0.000	0.000	0.000	0.000	0.000
	3.6-<3.8	0.000	0.000	0.000	0.000	0.000	0.000	0.000	0.000	0.000	0.000	0.000	0.000	0.000	0.000
	3.8<-3.0	0.000	0.000	0.000	0.000	0.000	0.000	0.000	0.000	0.000	0.000	0.000	0.000	0.000	0.000
	4.0-<4.2	0.000	0.000	0.000	0.000	0.000	0.000	0.000	0.000	0.000	0.000	0.000	0.000	0.000	0.000
	4.2-<4.4	0.000	0.000	0.000	0.000	0.000	0.000	0.000	0.000	0.000	0.000	0.000	0.000	0.000	0.000
	4.4-<4.6	0.000	0.000	0.000	0.000	0.000	0.000	0.000	0.000	0.000	0.000	0.000	0.000	0.000	0.000
	4.6-<4.8	0.000	0.000	0.000	0.000	0.000	0.000	0.000	0.000	0.000	0.000	0.000	0.000	0.000	0.000
	4.8-<5.0	0.000	0.000	0.000	0.000	0.000	0.000	0.000	0.000	0.000	0.000	0.000	0.000	0.000	0.000
	4.0-<5.2	0.000	0.000	0.000	0.000	0.000	0.000	0.000	0.000	0.000	0.000	0.000	0.000	0.000	0.000
	5.2-<5.4	0.000	0.000	0.000	0.000	0.000	0.000	0.000	0.000	0.000	0.000	0.000	0.000	0.000	0.000

	5.4-<5.6	0.000	0.000	0.000	0.000	0.000	0.000	0.000	0.000	0.000	0.000	0.000	0.000	0.000	0.000
	5.6-<5.8	0.000	0.000	0.000	0.000	0.000	0.000	0.000	0.000	0.000	0.000	0.000	0.000	0.000	0.000
	5.8-<6.0	0.000	0.000	0.000	0.000	0.000	0.000	0.000	0.000	0.000	0.000	0.000	0.000	0.000	0.000

		Incident Energy/MeV													
		3.4	3.6	3.8	4.0	4.2	4.4	4.6	4.8	5.0	5.2	5.4	5.6	5.8	6.0
Detected Energy/MeV	0-<0.2	0.000	0.000	0.000	0.000	0.000	0.000	0.000	0.000	0.000	0.000	0.000	0.000	0.000	0.000
	0.2-<0.4	0.000	0.000	0.000	0.000	0.000	0.000	0.000	0.000	0.000	0.000	0.000	0.000	0.000	0.000
	0.4-<0.6	0.000	0.000	0.000	0.000	0.000	0.000	0.000	0.000	0.000	0.000	0.000	0.000	0.000	0.000
	0.6-<0.8	0.000	0.000	0.000	0.000	0.000	0.000	0.000	0.000	0.000	0.000	0.000	0.000	0.000	0.000
	0.8-<1.0	0.000	0.000	0.000	0.000	0.000	0.000	0.000	0.000	0.000	0.000	0.000	0.000	0.000	0.000
	1.0-<1.2	0.000	0.000	0.000	0.000	0.000	0.000	0.000	0.000	0.000	0.000	0.000	0.000	0.000	0.000
	1.2-<1.4	0.000	0.000	0.000	0.000	0.000	0.000	0.000	0.000	0.000	0.000	0.000	0.000	0.000	0.000
	1.4-<1.6	0.000	0.000	0.000	0.000	0.000	0.000	0.000	0.000	0.000	0.000	0.000	0.000	0.000	0.000
	1.6-<1.8	0.000	0.000	0.000	0.000	0.000	0.000	0.000	0.000	0.000	0.000	0.000	0.000	0.000	0.000
	1.8-<2.0	0.000	0.000	0.000	0.000	0.000	0.000	0.000	0.000	0.000	0.000	0.000	0.000	0.000	0.000
	2.0-<2.2	0.000	0.000	0.000	0.001	0.000	0.000	0.000	0.000	0.000	0.000	0.000	0.000	0.000	0.000
	2.2-<2.4	0.000	0.000	0.000	0.000	0.000	0.000	0.000	0.000	0.000	0.000	0.000	0.000	0.000	0.029
	2.4-<2.6	0.000	0.010	0.029	0.000	0.000	0.057	0.000	0.001	0.011	0.000	0.019	0.019	0.058	0.001
	2.6-<2.8	0.000	0.029	0.000	0.000	0.000	0.000	0.058	0.000	0.128	0.000	0.000	0.038	0.001	0.029
	2.8-<3.0	0.020	0.047	0.020	0.000	0.085	0.030	0.094	0.089	0.058	0.099	0.088	0.029	0.085	0.127
	3.0-<3.2	0.000	0.049	0.000	0.000	0.067	0.039	0.038	0.039	0.020	0.057	0.079	0.031	0.094	0.086
	3.2-<3.4	0.702	0.159	0.020	0.140	0.031	0.147	0.123	0.126	0.153	0.150	0.179	0.152	0.042	0.144
	3.4-<3.6	0.445	0.856	0.284	0.077	0.093	0.099	0.140	0.115	0.068	0.030	0.176	0.095	0.039	0.136
	3.6-<3.8	0.000	0.246	1.016	0.192	0.161	0.020	0.060	0.069	0.086	0.106	0.099	0.039	0.114	0.117
	3.8<-3.0	0.000	0.000	0.601	1.400	0.134	0.210	0.030	0.077	0.031	0.130	0.135	0.049	0.059	0.116
	4.0-<4.2	0.000	0.000	0.000	0.425	0.705	0.059	0.096	0.080	0.143	0.229	0.020	0.076	0.057	0.011
	4.2-<4.4	0.000	0.000	0.000	0.000	0.604	0.762	0.231	0.089	0.069	0.001	0.029	0.049	0.020	0.020
	4.4-<4.6	0.000	0.000	0.000	0.000	0.000	0.496	0.846	0.107	0.020	0.057	0.048	0.076	0.040	0.135
	4.6-<4.8	0.000	0.000	0.000	0.000	0.000	0.000	0.570	1.078	0.201	0.060	0.050	0.060	0.011	0.131
	4.8-<5.0	0.000	0.000	0.000	0.000	0.000	0.000	0.000	0.384	0.482	0.088	0.174	0.079	0.010	0.050
	4.0-<5.2	0.000	0.000	0.000	0.000	0.000	0.000	0.000	0.000	0.646	0.539	0.165	0.049	0.060	0.114
	5.2-<5.4	0.000	0.000	0.000	0.000	0.000	0.000	0.000	0.000	0.000	0.335	0.352	0.078	0.106	0.039
	5.4-<5.6	0.000	0.000	0.000	0.000	0.000	0.000	0.000	0.000	0.000	0.000	0.176	0.518	0.050	0.069

	5.6-<5.8	0.000	0.000	0.000	0.000	0.000	0.000	0.000	0.000	0.000	0.000	0.000	0.191	0.667	0.135
	5.8-<6.0	0.000	0.000	0.000	0.000	0.000	0.000	0.000	0.000	0.000	0.000	0.000	0.000	0.186	0.276

B. Full Model

Total Events

		Incident Energy/MeV													
		0.6	0.8	1.0	1.2	1.4	1.6	1.8	2.0	2.2	2.4	2.6	2.8	3.0	3.2
Detected Energy/MeV	0-<0.2	0.000	0.000	0.000	0.000	0.000	0.000	0.000	0.000	0.000	0.000	0.000	0.000	0.000	0.000
	0.2-<0.4	0.000	0.000	0.000	0.000	0.000	0.000	0.058	0.000	0.001	0.038	0.067	0.000	0.000	0.048
	0.4-<0.6	0.019	0.000	0.107	0.277	0.085	0.176	0.246	0.039	0.196	0.229	0.020	0.362	0.075	0.136
	0.6-<0.8	0.000	0.638	0.056	0.362	0.287	0.040	0.203	0.375	0.155	0.170	0.315	0.115	0.010	0.076
	0.8-<1.0	0.000	0.000	1.634	0.454	0.591	0.721	0.379	0.413	0.141	0.348	0.396	0.105	0.021	0.011
	1.0-<1.2	0.000	0.000	0.000	2.840	0.493	0.391	0.496	0.153	0.322	0.283	0.340	0.186	0.049	0.252
	1.2-<1.4	0.000	0.000	0.000	0.000	3.899	0.551	0.409	0.202	0.467	0.467	0.264	0.517	0.208	0.256
	1.4-<1.6	0.000	0.000	0.000	0.000	0.000	4.218	0.418	0.354	1.135	0.464	0.086	0.337	0.153	0.371
	1.6-<1.8	0.000	0.000	0.000	0.000	0.000	0.000	5.365	0.520	0.823	0.320	0.343	0.502	0.107	0.223
	1.8-<2.0	0.000	0.000	0.000	0.000	0.000	0.000	0.000	3.917	0.797	0.512	0.378	0.320	0.184	0.305
	2.0-<2.2	0.000	0.000	0.000	0.000	0.000	0.000	0.000	0.000	6.466	1.035	0.828	0.602	0.302	0.273
	2.2-<2.4	0.000	0.000	0.000	0.000	0.000	0.000	0.000	0.000	0.000	6.671	1.000	0.404	0.369	0.441
	2.4-<2.6	0.000	0.000	0.000	0.000	0.000	0.000	0.000	0.000	0.000	0.000	6.107	0.641	0.181	0.489
	2.6-<2.8	0.000	0.000	0.000	0.000	0.000	0.000	0.000	0.000	0.000	0.000	0.000	5.636	0.485	0.441
	2.8-<3.0	0.000	0.000	0.000	0.000	0.000	0.000	0.000	0.000	0.000	0.000	0.000	0.000	3.635	0.564
	3.0-<3.2	0.000	0.000	0.000	0.000	0.000	0.000	0.000	0.000	0.000	0.000	0.000	0.000	0.000	6.415
	3.2-<3.4	0.000	0.000	0.000	0.000	0.000	0.000	0.000	0.000	0.000	0.000	0.000	0.000	0.000	0.000
	3.4-<3.6	0.000	0.000	0.000	0.000	0.000	0.000	0.000	0.000	0.000	0.000	0.000	0.000	0.000	0.000
	3.6-<3.8	0.000	0.000	0.000	0.000	0.000	0.000	0.000	0.000	0.000	0.000	0.000	0.000	0.000	0.000
	3.8<-3.0	0.000	0.000	0.000	0.000	0.000	0.000	0.000	0.000	0.000	0.000	0.000	0.000	0.000	0.000
	4.0-<4.2	0.000	0.000	0.000	0.000	0.000	0.000	0.000	0.000	0.000	0.000	0.000	0.000	0.000	0.000
	4.2-<4.4	0.000	0.000	0.000	0.000	0.000	0.000	0.000	0.000	0.000	0.000	0.000	0.000	0.000	0.000
	4.4-<4.6	0.000	0.000	0.000	0.000	0.000	0.000	0.000	0.000	0.000	0.000	0.000	0.000	0.000	0.000
	4.6-<4.8	0.000	0.000	0.000	0.000	0.000	0.000	0.000	0.000	0.000	0.000	0.000	0.000	0.000	0.000
	4.8-<5.0	0.000	0.000	0.000	0.000	0.000	0.000	0.000	0.000	0.000	0.000	0.000	0.000	0.000	0.000

	4.0-<5.2	0.000	0.000	0.000	0.000	0.000	0.000	0.000	0.000	0.000	0.000	0.000	0.000	0.000	0.000
	5.2-<5.4	0.000	0.000	0.000	0.000	0.000	0.000	0.000	0.000	0.000	0.000	0.000	0.000	0.000	0.000
	5.4-<5.6	0.000	0.000	0.000	0.000	0.000	0.000	0.000	0.000	0.000	0.000	0.000	0.000	0.000	0.000
	5.6-<5.8	0.000	0.000	0.000	0.000	0.000	0.000	0.000	0.000	0.000	0.000	0.000	0.000	0.000	0.000
	5.8-<6.0	0.000	0.000	0.000	0.000	0.000	0.000	0.000	0.000	0.000	0.000	0.000	0.000	0.000	0.000

		Incident Energy/MeV													
		3.4	3.6	3.8	4.0	4.2	4.4	4.6	4.8	5.0	5.2	5.4	5.6	5.8	6.0
Detected Energy/MeV	0-<0.2	0.000	0.000	0.000	0.000	0.000	0.000	0.000	0.000	0.000	0.000	0.001	0.000	0.000	0.000
	0.2-<0.4	0.001	0.000	0.010	0.000	0.000	0.000	0.064	0.001	0.064	0.000	0.047	0.000	0.047	0.000
	0.4-<0.6	0.298	0.010	0.095	0.000	0.038	0.111	0.001	0.000	0.010	0.103	0.000	0.010	0.000	0.000
	0.6-<0.8	0.074	0.030	0.126	0.020	0.001	0.029	0.000	0.074	0.000	0.067	0.112	0.224	0.101	0.010
	0.8-<1.0	0.206	0.152	0.076	0.029	0.072	0.000	0.079	0.038	0.000	0.110	0.175	0.019	0.072	0.000
	1.0-<1.2	0.146	0.191	0.144	0.019	0.074	0.000	0.019	0.118	0.056	0.094	0.000	0.000	0.038	0.010
	1.2-<1.4	0.320	0.266	0.179	0.030	0.000	0.157	0.086	0.038	0.000	0.047	0.152	0.029	0.143	0.010
	1.4-<1.6	0.274	0.182	0.249	0.058	0.218	0.057	0.076	0.067	0.001	0.212	0.048	0.193	0.067	0.058
	1.6-<1.8	0.173	0.195	0.316	0.106	0.127	0.049	0.125	0.272	0.101	0.146	0.048	0.091	0.088	0.064
	1.8-<2.0	0.323	0.247	0.113	0.160	0.269	0.172	0.098	0.042	0.019	0.059	0.089	0.151	0.089	0.095
	2.0-<2.2	0.263	0.330	0.155	0.221	0.212	0.236	0.429	0.209	0.068	0.070	0.289	0.231	0.115	0.001
	2.2-<2.4	0.355	0.333	0.422	0.126	0.130	0.157	0.263	0.143	0.145	0.125	0.173	0.155	0.183	0.127
	2.4-<2.6	0.455	0.457	0.379	0.151	0.371	0.194	0.174	0.105	0.088	0.197	0.333	0.291	0.366	0.207
	2.6-<2.8	0.378	0.319	0.354	0.271	0.405	0.477	0.412	0.596	0.197	0.572	0.609	0.537	0.764	0.495
	2.8-<3.0	0.956	0.622	0.443	0.164	0.533	0.639	0.678	0.568	0.487	0.844	0.952	1.175	1.137	0.797
	3.0-<3.2	0.888	0.509	0.416	0.366	0.539	0.854	0.675	0.933	0.517	0.495	0.786	0.999	1.451	0.743
	3.2-<3.4	7.232	1.049	0.721	0.228	0.714	0.608	0.818	0.733	0.569	1.376	0.798	1.224	0.857	0.507
	3.4-<3.6	0.000	5.818	0.868	0.584	0.753	0.855	0.719	0.469	0.269	0.456	0.830	0.662	1.086	0.334
	3.6-<3.8	0.000	0.000	5.908	0.655	0.333	0.552	0.773	0.724	0.486	0.687	0.778	0.765	0.726	0.372
	3.8<-3.0	0.000	0.000	0.000	3.579	1.132	0.819	0.744	0.540	0.301	0.490	0.393	0.594	0.713	0.474
	4.0-<4.2	0.000	0.000	0.000	0.000	4.877	0.514	0.725	0.532	0.233	0.524	0.561	0.564	0.717	0.404
	4.2-<4.4	0.000	0.000	0.000	0.000	0.000	4.440	1.094	0.499	0.261	0.661	0.447	0.395	0.542	0.259
	4.4-<4.6	0.000	0.000	0.000	0.000	0.000	0.000	3.886	0.781	0.299	0.352	0.266	0.336	0.502	0.325
	4.6-<4.8	0.000	0.000	0.000	0.000	0.000	0.000	0.000	3.157	0.208	0.543	0.451	0.405	0.370	0.387
	4.8-<5.0	0.000	0.000	0.000	0.000	0.000	0.000	0.000	0.000	1.250	0.565	0.390	0.591	0.360	0.137
	4.0-<5.2	0.000	0.000	0.000	0.000	0.000	0.000	0.000	0.000	0.000	2.090	0.443	0.379	0.256	0.079

	5.2-<5.4	0.000	0.000	0.000	0.000	0.000	0.000	0.000	0.000	0.000	0.000	1.641	0.320	0.273	0.106
	5.4-<5.6	0.000	0.000	0.000	0.000	0.000	0.000	0.000	0.000	0.000	0.000	0.000	1.070	0.367	0.296
	5.6-<5.8	0.000	0.000	0.000	0.000	0.000	0.000	0.000	0.000	0.000	0.000	0.000	0.000	0.914	0.147
	5.8-<6.0	0.000	0.000	0.000	0.000	0.000	0.000	0.000	0.000	0.000	0.000	0.000	0.000	0.000	0.458

R2 Events

		Incident Energy/MeV													
		0.6	0.8	1.0	1.2	1.4	1.6	1.8	2.0	2.2	2.4	2.6	2.8	3.0	3.2
Detected Energy/MeV	0-<0.2	0.000	0.000	0.000	0.000	0.000	0.000	0.000	0.000	0.000	0.000	0.000	0.000	0.000	0.000
	0.2-<0.4	0.000	0.000	0.000	0.000	0.000	0.000	0.001	0.000	0.000	0.000	0.020	0.000	0.000	0.048
	0.4-<0.6	0.000	0.000	0.107	0.219	0.085	0.066	0.086	0.039	0.047	0.181	0.000	0.245	0.075	0.064
	0.6-<0.8	0.000	0.280	0.056	0.235	0.029	0.020	0.092	0.327	0.030	0.075	0.243	0.115	0.010	0.076
	0.8-<1.0	0.000	0.000	1.634	0.105	0.208	0.369	0.198	0.354	0.000	0.068	0.220	0.029	0.001	0.010
	1.0-<1.2	0.000	0.000	0.000	1.619	0.210	0.077	0.218	0.057	0.120	0.123	0.000	0.108	0.010	0.184
	1.2-<1.4	0.000	0.000	0.000	0.000	1.516	0.210	0.029	0.050	0.029	0.082	0.105	0.047	0.067	0.096
	1.4-<1.6	0.000	0.000	0.000	0.000	0.000	1.114	0.140	0.177	0.283	0.094	0.047	0.000	0.047	0.010
	1.6-<1.8	0.000	0.000	0.000	0.000	0.000	0.000	0.582	0.150	0.158	0.000	0.066	0.056	0.000	0.019
	1.8-<2.0	0.000	0.000	0.000	0.000	0.000	0.000	0.000	0.187	0.000	0.000	0.083	0.038	0.038	0.019
	2.0-<2.2	0.000	0.000	0.000	0.000	0.000	0.000	0.000	0.000	0.059	0.000	0.000	0.010	0.072	0.000
	2.2-<2.4	0.000	0.000	0.000	0.000	0.000	0.000	0.000	0.000	0.000	0.047	0.000	0.000	0.000	0.000
	2.4-<2.6	0.000	0.000	0.000	0.000	0.000	0.000	0.000	0.000	0.000	0.000	0.048	0.000	0.000	0.000
	2.6-<2.8	0.000	0.000	0.000	0.000	0.000	0.000	0.000	0.000	0.000	0.000	0.000	0.072	0.000	0.000
	2.8-<3.0	0.000	0.000	0.000	0.000	0.000	0.000	0.000	0.000	0.000	0.000	0.000	0.000	0.000	0.000
	3.0-<3.2	0.000	0.000	0.000	0.000	0.000	0.000	0.000	0.000	0.000	0.000	0.000	0.000	0.000	0.000
	3.2-<3.4	0.000	0.000	0.000	0.000	0.000	0.000	0.000	0.000	0.000	0.000	0.000	0.000	0.000	0.000
	3.4-<3.6	0.000	0.000	0.000	0.000	0.000	0.000	0.000	0.000	0.000	0.000	0.000	0.000	0.000	0.000
	3.6-<3.8	0.000	0.000	0.000	0.000	0.000	0.000	0.000	0.000	0.000	0.000	0.000	0.000	0.000	0.000
	3.8<-3.0	0.000	0.000	0.000	0.000	0.000	0.000	0.000	0.000	0.000	0.000	0.000	0.000	0.000	0.000
	4.0-<4.2	0.000	0.000	0.000	0.000	0.000	0.000	0.000	0.000	0.000	0.000	0.000	0.000	0.000	0.000
	4.2-<4.4	0.000	0.000	0.000	0.000	0.000	0.000	0.000	0.000	0.000	0.000	0.000	0.000	0.000	0.000
	4.4-<4.6	0.000	0.000	0.000	0.000	0.000	0.000	0.000	0.000	0.000	0.000	0.000	0.000	0.000	0.000
	4.6-<4.8	0.000	0.000	0.000	0.000	0.000	0.000	0.000	0.000	0.000	0.000	0.000	0.000	0.000	0.000
	4.8-<5.0	0.000	0.000	0.000	0.000	0.000	0.000	0.000	0.000	0.000	0.000	0.000	0.000	0.000	0.000

	4.0-<5.2	0.000	0.000	0.000	0.000	0.000	0.000	0.000	0.000	0.000	0.000	0.000	0.000	0.000	0.000
	5.2-<5.4	0.000	0.000	0.000	0.000	0.000	0.000	0.000	0.000	0.000	0.000	0.000	0.000	0.000	0.000
	5.4-<5.6	0.000	0.000	0.000	0.000	0.000	0.000	0.000	0.000	0.000	0.000	0.000	0.000	0.000	0.000
	5.6-<5.8	0.000	0.000	0.000	0.000	0.000	0.000	0.000	0.000	0.000	0.000	0.000	0.000	0.000	0.000
	5.8-<6.0	0.000	0.000	0.000	0.000	0.000	0.000	0.000	0.000	0.000	0.000	0.000	0.000	0.000	0.000

		Incident Energy/MeV													
		3.4	3.6	3.8	4.0	4.2	4.4	4.6	4.8	5.0	5.2	5.4	5.6	5.8	6.0
Detected Energy/MeV	0-<0.2	0.000	0.000	0.000	0.000	0.000	0.000	0.000	0.000	0.000	0.000	0.000	0.001	0.000	0.000
	0.2-<0.4	0.048	0.000	0.000	0.010	0.000	0.000	0.000	0.000	0.001	0.064	0.000	0.000	0.000	0.000
	0.4-<0.6	0.064	0.242	0.000	0.076	0.000	0.000	0.000	0.001	0.000	0.010	0.000	0.000	0.010	0.000
	0.6-<0.8	0.076	0.000	0.000	0.079	0.020	0.000	0.000	0.000	0.074	0.000	0.000	0.000	0.168	0.072
	0.8-<1.0	0.010	0.029	0.001	0.038	0.000	0.072	0.000	0.000	0.000	0.000	0.000	0.097	0.000	0.000
	1.0-<1.2	0.184	0.076	0.057	0.072	0.019	0.064	0.000	0.000	0.079	0.000	0.000	0.000	0.000	0.038
	1.2-<1.4	0.096	0.010	0.000	0.102	0.000	0.000	0.000	0.000	0.000	0.000	0.047	0.086	0.000	0.143
	1.4-<1.6	0.010	0.000	0.056	0.064	0.000	0.000	0.000	0.000	0.000	0.000	0.000	0.000	0.079	0.010
	1.6-<1.8	0.019	0.000	0.019	0.000	0.000	0.000	0.000	0.056	0.064	0.000	0.000	0.000	0.000	0.000
	1.8-<2.0	0.019	0.056	0.000	0.000	0.000	0.000	0.000	0.000	0.000	0.000	0.000	0.000	0.056	0.000
	2.0-<2.2	0.000	0.000	0.064	0.000	0.000	0.000	0.000	0.000	0.000	0.000	0.000	0.000	0.000	0.000
	2.2-<2.4	0.000	0.000	0.091	0.000	0.000	0.000	0.000	0.000	0.000	0.000	0.000	0.000	0.000	0.000
	2.4-<2.6	0.000	0.000	0.029	0.000	0.000	0.000	0.000	0.000	0.000	0.000	0.000	0.000	0.000	0.000
	2.6-<2.8	0.000	0.000	0.000	0.000	0.000	0.000	0.000	0.000	0.000	0.000	0.000	0.000	0.000	0.000
	2.8-<3.0	0.000	0.000	0.000	0.000	0.000	0.000	0.000	0.000	0.000	0.000	0.000	0.000	0.000	0.000
	3.0-<3.2	0.000	0.000	0.019	0.000	0.000	0.000	0.000	0.000	0.001	0.000	0.000	0.000	0.000	0.000
	3.2-<3.4	0.000	0.000	0.000	0.000	0.000	0.000	0.000	0.000	0.000	0.000	0.000	0.000	0.000	0.000
	3.4-<3.6	0.000	0.000	0.000	0.000	0.000	0.000	0.000	0.000	0.000	0.000	0.000	0.000	0.000	0.000
	3.6-<3.8	0.000	0.000	0.000	0.000	0.000	0.000	0.000	0.000	0.000	0.000	0.000	0.000	0.000	0.000
	3.8<-3.0	0.000	0.000	0.000	0.000	0.000	0.000	0.000	0.000	0.000	0.000	0.000	0.000	0.000	0.000
	4.0-<4.2	0.000	0.000	0.000	0.000	0.000	0.000	0.000	0.000	0.000	0.000	0.000	0.000	0.000	0.000
	4.2-<4.4	0.000	0.000	0.000	0.000	0.000	0.000	0.000	0.000	0.000	0.000	0.000	0.000	0.000	0.000
	4.4-<4.6	0.000	0.000	0.000	0.000	0.000	0.000	0.000	0.000	0.000	0.000	0.000	0.000	0.000	0.000
	4.6-<4.8	0.000	0.000	0.000	0.000	0.000	0.000	0.000	0.000	0.000	0.000	0.000	0.000	0.000	0.000
	4.8-<5.0	0.000	0.000	0.000	0.000	0.000	0.000	0.000	0.000	0.000	0.000	0.000	0.000	0.000	0.000
	4.0-<5.2	0.000	0.000	0.000	0.000	0.000	0.000	0.000	0.000	0.000	0.000	0.000	0.000	0.000	0.000

	5.2-<5.4	0.000	0.000	0.000	0.000	0.000	0.000	0.000	0.000	0.000	0.000	0.000	0.000	0.000	0.000
	5.4-<5.6	0.000	0.000	0.000	0.000	0.000	0.000	0.000	0.000	0.000	0.000	0.000	0.000	0.000	0.000
	5.6-<5.8	0.000	0.000	0.000	0.000	0.000	0.000	0.000	0.000	0.000	0.000	0.000	0.000	0.000	0.000
	5.8-<6.0	0.000	0.000	0.000	0.000	0.000	0.000	0.000	0.000	0.000	0.000	0.000	0.000	0.000	0.000

R3 Events

		Incident Energy/MeV													
		0.6	0.8	1.0	1.2	1.4	1.6	1.8	2.0	2.2	2.4	2.6	2.8	3.0	3.2
Detected Energy/MeV	0-<0.2	0.000	0.000	0.000	0.000	0.000	0.000	0.000	0.000	0.000	0.000	0.000	0.000	0.000	0.000
	0.2-<0.4	0.000	0.000	0.000	0.000	0.000	0.000	0.000	0.000	0.000	0.000	0.047	0.000	0.000	0.000
	0.4-<0.6	0.000	0.000	0.000	0.000	0.000	0.110	0.000	0.000	0.000	0.000	0.000	0.038	0.000	0.000
	0.6-<0.8	0.000	0.000	0.000	0.019	0.000	0.000	0.000	0.047	0.010	0.000	0.000	0.000	0.000	0.000
	0.8-<1.0	0.000	0.000	0.000	0.001	0.150	0.001	0.010	0.059	0.047	0.057	0.176	0.000	0.020	0.000
	1.0-<1.2	0.000	0.000	0.000	0.114	0.030	0.142	0.086	0.095	0.038	0.104	0.247	0.029	0.039	0.047
	1.2-<1.4	0.000	0.000	0.000	0.000	0.467	0.130	0.078	0.152	0.294	0.111	0.091	0.252	0.140	0.159
	1.4-<1.6	0.000	0.000	0.000	0.000	0.000	1.620	0.143	0.177	0.286	0.249	0.010	0.222	0.106	0.194
	1.6-<1.8	0.000	0.000	0.000	0.000	0.000	0.000	2.416	0.332	0.381	0.195	0.190	0.198	0.107	0.119
	1.8-<2.0	0.000	0.000	0.000	0.000	0.000	0.000	0.000	3.516	0.564	0.235	0.097	0.205	0.146	0.172
	2.0-<2.2	0.000	0.000	0.000	0.000	0.000	0.000	0.000	0.000	3.162	0.403	0.307	0.304	0.202	0.068
	2.2-<2.4	0.000	0.000	0.000	0.000	0.000	0.000	0.000	0.000	0.000	2.832	0.451	0.163	0.190	0.098
	2.4-<2.6	0.000	0.000	0.000	0.000	0.000	0.000	0.000	0.000	0.000	0.000	1.916	0.276	0.132	0.077
	2.6-<2.8	0.000	0.000	0.000	0.000	0.000	0.000	0.000	0.000	0.000	0.000	0.000	1.275	0.151	0.105
	2.8-<3.0	0.000	0.000	0.000	0.000	0.000	0.000	0.000	0.000	0.000	0.000	0.000	0.000	1.248	0.105
	3.0-<3.2	0.000	0.000	0.000	0.000	0.000	0.000	0.000	0.000	0.000	0.000	0.000	0.000	0.000	1.288
	3.2-<3.4	0.000	0.000	0.000	0.000	0.000	0.000	0.000	0.000	0.000	0.000	0.000	0.000	0.000	0.000
	3.4-<3.6	0.000	0.000	0.000	0.000	0.000	0.000	0.000	0.000	0.000	0.000	0.000	0.000	0.000	0.000
	3.6-<3.8	0.000	0.000	0.000	0.000	0.000	0.000	0.000	0.000	0.000	0.000	0.000	0.000	0.000	0.000
	3.8<-3.0	0.000	0.000	0.000	0.000	0.000	0.000	0.000	0.000	0.000	0.000	0.000	0.000	0.000	0.000
	4.0-<4.2	0.000	0.000	0.000	0.000	0.000	0.000	0.000	0.000	0.000	0.000	0.000	0.000	0.000	0.000
	4.2-<4.4	0.000	0.000	0.000	0.000	0.000	0.000	0.000	0.000	0.000	0.000	0.000	0.000	0.000	0.000
	4.4-<4.6	0.000	0.000	0.000	0.000	0.000	0.000	0.000	0.000	0.000	0.000	0.000	0.000	0.000	0.000
	4.6-<4.8	0.000	0.000	0.000	0.000	0.000	0.000	0.000	0.000	0.000	0.000	0.000	0.000	0.000	0.000
	4.8-<5.0	0.000	0.000	0.000	0.000	0.000	0.000	0.000	0.000	0.000	0.000	0.000	0.000	0.000	0.000

	4.0-<5.2	0.000	0.000	0.000	0.000	0.000	0.000	0.000	0.000	0.000	0.000	0.000	0.000	0.000	0.000
	5.2-<5.4	0.000	0.000	0.000	0.000	0.000	0.000	0.000	0.000	0.000	0.000	0.000	0.000	0.000	0.000
	5.4-<5.6	0.000	0.000	0.000	0.000	0.000	0.000	0.000	0.000	0.000	0.000	0.000	0.000	0.000	0.000
	5.6-<5.8	0.000	0.000	0.000	0.000	0.000	0.000	0.000	0.000	0.000	0.000	0.000	0.000	0.000	0.000
	5.8-<6.0	0.000	0.000	0.000	0.000	0.000	0.000	0.000	0.000	0.000	0.000	0.000	0.000	0.000	0.000

		Incident Energy/MeV													
		3.4	3.6	3.8	4.0	4.2	4.4	4.6	4.8	5.0	5.2	5.4	5.6	5.8	6.0
Detected Energy/MeV	0-<0.2	0.000	0.000	0.000	0.000	0.000	0.000	0.000	0.000	0.000	0.000	0.000	0.000	0.000	0.000
	0.2-<0.4	0.000	0.000	0.000	0.000	0.000	0.000	0.000	0.000	0.000	0.000	0.000	0.000	0.000	0.000
	0.4-<0.6	0.000	0.000	0.000	0.000	0.000	0.000	0.000	0.000	0.000	0.000	0.000	0.000	0.000	0.000
	0.6-<0.8	0.000	0.000	0.000	0.000	0.000	0.000	0.000	0.000	0.000	0.000	0.011	0.000	0.000	0.029
	0.8-<1.0	0.000	0.000	0.019	0.038	0.029	0.000	0.000	0.000	0.000	0.000	0.038	0.000	0.000	0.000
	1.0-<1.2	0.047	0.001	0.038	0.000	0.000	0.010	0.000	0.019	0.039	0.056	0.038	0.000	0.000	0.000
	1.2-<1.4	0.159	0.128	0.048	0.038	0.030	0.000	0.019	0.057	0.000	0.000	0.000	0.066	0.029	0.000
	1.4-<1.6	0.194	0.113	0.030	0.128	0.058	0.095	0.038	0.000	0.067	0.001	0.029	0.019	0.086	0.000
	1.6-<1.8	0.119	0.049	0.049	0.229	0.077	0.021	0.000	0.020	0.122	0.101	0.057	0.000	0.072	0.029
	1.8-<2.0	0.172	0.098	0.011	0.020	0.160	0.068	0.047	0.077	0.021	0.000	0.001	0.029	0.000	0.029
	2.0-<2.2	0.068	0.174	0.160	0.039	0.219	0.068	0.057	0.324	0.094	0.029	0.029	0.211	0.000	0.029
	2.2-<2.4	0.098	0.133	0.162	0.139	0.047	0.001	0.135	0.040	0.010	0.069	0.058	0.000	0.048	0.000
	2.4-<2.6	0.077	0.218	0.107	0.140	0.150	0.115	0.069	0.001	0.000	0.019	0.030	0.048	0.000	0.000
	2.6-<2.8	0.105	0.056	0.097	0.102	0.152	0.000	0.001	0.039	0.020	0.019	0.000	0.094	0.000	0.000
	2.8-<3.0	0.105	0.341	0.160	0.125	0.030	0.039	0.039	0.020	0.076	0.010	0.057	0.039	0.000	0.000
	3.0-<3.2	1.288	0.180	0.049	0.020	0.175	0.059	0.131	0.058	0.057	0.031	0.000	0.001	0.000	0.047
	3.2-<3.4	0.000	0.610	0.048	0.001	0.010	0.117	0.038	0.135	0.121	0.001	0.066	0.038	0.048	0.029
	3.4-<3.6	0.000	0.000	0.615	0.181	0.084	0.067	0.079	0.066	0.000	0.000	0.000	0.010	0.000	0.000
	3.6-<3.8	0.000	0.000	0.000	0.243	0.096	0.000	0.019	0.001	0.047	0.074	0.029	0.000	0.000	0.064
	3.8<-3.0	0.000	0.000	0.000	0.000	0.261	0.030	0.077	0.000	0.000	0.010	0.001	0.000	0.011	0.000
	4.0-<4.2	0.000	0.000	0.000	0.000	0.000	0.412	0.000	0.000	0.000	0.069	0.001	0.000	0.048	0.029
	4.2-<4.4	0.000	0.000	0.000	0.000	0.000	0.000	0.200	0.066	0.000	0.038	0.000	0.000	0.000	0.056
	4.4-<4.6	0.000	0.000	0.000	0.000	0.000	0.000	0.000	0.040	0.011	0.001	0.011	0.001	0.000	0.000
	4.6-<4.8	0.000	0.000	0.000	0.000	0.000	0.000	0.000	0.000	0.057	0.001	0.000	0.000	0.038	0.019
	4.8-<5.0	0.000	0.000	0.000	0.000	0.000	0.000	0.000	0.000	0.000	0.085	0.000	0.000	0.000	0.000
	4.0-<5.2	0.000	0.000	0.000	0.000	0.000	0.000	0.000	0.000	0.000	0.000	0.111	0.010	0.000	0.038

	5.2-<5.4	0.000	0.000	0.000	0.000	0.000	0.000	0.000	0.000	0.000	0.000	0.000	0.000	0.000	0.000
	5.4-<5.6	0.000	0.000	0.000	0.000	0.000	0.000	0.000	0.000	0.000	0.000	0.000	0.000	0.000	0.010
	5.6-<5.8	0.000	0.000	0.000	0.000	0.000	0.000	0.000	0.000	0.000	0.000	0.000	0.000	0.000	0.000
	5.8-<6.0	0.000	0.000	0.000	0.000	0.000	0.000	0.000	0.000	0.000	0.000	0.000	0.000	0.000	0.000

R4 Events

		Incident Energy/MeV													
		0.6	0.8	1.0	1.2	1.4	1.6	1.8	2.0	2.2	2.4	2.6	2.8	3.0	3.2
Detected Energy/MeV	0-<0.2	0.000	0.000	0.000	0.000	0.000	0.000	0.000	0.000	0.000	0.000	0.000	0.000	0.000	0.000
	0.2-<0.4	0.000	0.000	0.000	0.000	0.000	0.000	0.000	0.000	0.000	0.000	0.000	0.000	0.000	0.000
	0.4-<0.6	0.000	0.000	0.000	0.000	0.000	0.000	0.000	0.000	0.000	0.000	0.000	0.000	0.000	0.000
	0.6-<0.8	0.000	0.000	0.000	0.000	0.000	0.000	0.000	0.000	0.000	0.000	0.000	0.000	0.000	0.000
	0.8-<1.0	0.000	0.000	0.000	0.000	0.001	0.001	0.000	0.000	0.000	0.000	0.000	0.000	0.000	0.000
	1.0-<1.2	0.000	0.000	0.000	0.000	0.000	0.000	0.000	0.000	0.000	0.000	0.000	0.000	0.000	0.000
	1.2-<1.4	0.000	0.000	0.000	0.000	0.000	0.000	0.000	0.000	0.000	0.000	0.000	0.000	0.001	0.000
	1.4-<1.6	0.000	0.000	0.000	0.000	0.000	0.000	0.000	0.000	0.000	0.000	0.000	0.000	0.000	0.000
	1.6-<1.8	0.000	0.000	0.000	0.000	0.000	0.000	0.030	0.000	0.000	0.000	0.000	0.098	0.000	0.000
	1.8-<2.0	0.000	0.000	0.000	0.000	0.000	0.000	0.000	0.143	0.000	0.086	0.000	0.029	0.000	0.029
	2.0-<2.2	0.000	0.000	0.000	0.000	0.000	0.000	0.000	0.000	0.548	0.113	0.057	0.072	0.029	0.066
	2.2-<2.4	0.000	0.000	0.000	0.000	0.000	0.000	0.000	0.000	0.000	0.996	0.124	0.011	0.179	0.056
	2.4-<2.6	0.000	0.000	0.000	0.000	0.000	0.000	0.000	0.000	0.000	0.000	1.543	0.199	0.049	0.190
	2.6-<2.8	0.000	0.000	0.000	0.000	0.000	0.000	0.000	0.000	0.000	0.000	0.000	1.707	0.267	0.089
	2.8-<3.0	0.000	0.000	0.000	0.000	0.000	0.000	0.000	0.000	0.000	0.000	0.000	0.000	1.980	0.162
	3.0-<3.2	0.000	0.000	0.000	0.000	0.000	0.000	0.000	0.000	0.000	0.000	0.000	0.000	0.000	2.540
	3.2-<3.4	0.000	0.000	0.000	0.000	0.000	0.000	0.000	0.000	0.000	0.000	0.000	0.000	0.000	0.000
	3.4-<3.6	0.000	0.000	0.000	0.000	0.000	0.000	0.000	0.000	0.000	0.000	0.000	0.000	0.000	0.000
	3.6-<3.8	0.000	0.000	0.000	0.000	0.000	0.000	0.000	0.000	0.000	0.000	0.000	0.000	0.000	0.000
	3.8<-3.0	0.000	0.000	0.000	0.000	0.000	0.000	0.000	0.000	0.000	0.000	0.000	0.000	0.000	0.000
	4.0-<4.2	0.000	0.000	0.000	0.000	0.000	0.000	0.000	0.000	0.000	0.000	0.000	0.000	0.000	0.000
	4.2-<4.4	0.000	0.000	0.000	0.000	0.000	0.000	0.000	0.000	0.000	0.000	0.000	0.000	0.000	0.000
	4.4-<4.6	0.000	0.000	0.000	0.000	0.000	0.000	0.000	0.000	0.000	0.000	0.000	0.000	0.000	0.000
	4.6-<4.8	0.000	0.000	0.000	0.000	0.000	0.000	0.000	0.000	0.000	0.000	0.000	0.000	0.000	0.000
	4.8-<5.0	0.000	0.000	0.000	0.000	0.000	0.000	0.000	0.000	0.000	0.000	0.000	0.000	0.000	0.000

	4.0-<5.2	0.000	0.000	0.000	0.000	0.000	0.000	0.000	0.000	0.000	0.000	0.000	0.000	0.000	0.000
	5.2-<5.4	0.000	0.000	0.000	0.000	0.000	0.000	0.000	0.000	0.000	0.000	0.000	0.000	0.000	0.000
	5.4-<5.6	0.000	0.000	0.000	0.000	0.000	0.000	0.000	0.000	0.000	0.000	0.000	0.000	0.000	0.000
	5.6-<5.8	0.000	0.000	0.000	0.000	0.000	0.000	0.000	0.000	0.000	0.000	0.000	0.000	0.000	0.000
	5.8-<6.0	0.000	0.000	0.000	0.000	0.000	0.000	0.000	0.000	0.000	0.000	0.000	0.000	0.000	0.000

		Incident Energy/MeV													
		3.4	3.6	3.8	4.0	4.2	4.4	4.6	4.8	5.0	5.2	5.4	5.6	5.8	6.0
Detected Energy/MeV	0-<0.2	0.000	0.000	0.000	0.000	0.000	0.000	0.000	0.000	0.000	0.000	0.000	0.000	0.000	0.000
	0.2-<0.4	0.000	0.000	0.000	0.000	0.000	0.000	0.000	0.000	0.000	0.000	0.000	0.000	0.000	0.000
	0.4-<0.6	0.000	0.000	0.000	0.000	0.000	0.000	0.000	0.000	0.000	0.000	0.000	0.000	0.000	0.000
	0.6-<0.8	0.000	0.000	0.000	0.000	0.000	0.000	0.000	0.000	0.000	0.000	0.000	0.000	0.000	0.000
	0.8-<1.0	0.000	0.000	0.000	0.000	0.000	0.000	0.000	0.000	0.000	0.000	0.000	0.000	0.000	0.000
	1.0-<1.2	0.000	0.000	0.000	0.000	0.000	0.000	0.000	0.000	0.000	0.000	0.000	0.000	0.000	0.000
	1.2-<1.4	0.000	0.000	0.000	0.000	0.000	0.000	0.000	0.000	0.000	0.000	0.000	0.000	0.000	0.000
	1.4-<1.6	0.000	0.056	0.000	0.000	0.000	0.000	0.019	0.000	0.000	0.000	0.038	0.000	0.000	0.000
	1.6-<1.8	0.000	0.000	0.056	0.029	0.029	0.000	0.020	0.019	0.000	0.000	0.010	0.000	0.000	0.010
	1.8-<2.0	0.029	0.168	0.093	0.001	0.000	0.000	0.086	0.000	0.021	0.019	0.048	0.020	0.095	0.030
	2.0-<2.2	0.066	0.029	0.001	0.000	0.002	0.019	0.077	0.057	0.020	0.039	0.041	0.078	0.000	0.086
	2.2-<2.4	0.056	0.163	0.010	0.144	0.041	0.088	0.002	0.125	0.048	0.029	0.019	0.058	0.030	0.059
	2.4-<2.6	0.190	0.020	0.102	0.144	0.001	0.159	0.019	0.096	0.075	0.068	0.059	0.047	0.020	0.010
	2.6-<2.8	0.089	0.112	0.115	0.030	0.020	0.048	0.165	0.105	0.029	0.068	0.056	0.160	0.064	0.114
	2.8-<3.0	0.162	0.388	0.139	0.058	0.105	0.087	0.167	0.113	0.001	0.166	0.112	0.144	0.048	0.189
	3.0-<3.2	2.540	0.236	0.150	0.048	0.113	0.105	0.115	0.150	0.104	0.114	0.134	0.068	0.135	0.000
	3.2-<3.4	0.000	2.406	0.152	0.287	0.161	0.077	0.145	0.134	0.069	0.076	0.126	0.029	0.095	0.021
	3.4-<3.6	0.000	0.000	2.035	0.116	0.232	0.172	0.266	0.169	0.069	0.030	0.000	0.029	0.001	0.068
	3.6-<3.8	0.000	0.000	0.000	1.713	0.432	0.128	0.079	0.162	0.057	0.209	0.000	0.059	0.049	0.019
	3.8<-3.0	0.000	0.000	0.000	0.000	1.814	0.309	0.108	0.019	0.105	0.011	0.029	0.030	0.010	0.010
	4.0-<4.2	0.000	0.000	0.000	0.000	0.000	0.827	0.117	0.115	0.067	0.011	0.077	0.072	0.011	0.000
	4.2-<4.4	0.000	0.000	0.000	0.000	0.000	0.000	1.334	0.204	0.030	0.066	0.068	0.102	0.038	0.077
	4.4-<4.6	0.000	0.000	0.000	0.000	0.000	0.000	0.000	0.553	0.163	0.087	0.030	0.049	0.076	0.039
	4.6-<4.8	0.000	0.000	0.000	0.000	0.000	0.000	0.000	0.000	0.899	0.032	0.122	0.038	0.001	0.001
	4.8-<5.0	0.000	0.000	0.000	0.000	0.000	0.000	0.000	0.000	0.000	0.569	0.124	0.068	0.105	0.000
	4.0-<5.2	0.000	0.000	0.000	0.000	0.000	0.000	0.000	0.000	0.000	0.000	0.527	0.066	0.001	0.001

	5.2-<5.4	0.000	0.000	0.000	0.000	0.000	0.000	0.000	0.000	0.000	0.000	0.000	0.243	0.048	0.011
	5.4-<5.6	0.000	0.000	0.000	0.000	0.000	0.000	0.000	0.000	0.000	0.000	0.000	0.000	0.166	0.040
	5.6-<5.8	0.000	0.000	0.000	0.000	0.000	0.000	0.000	0.000	0.000	0.000	0.000	0.000	0.000	0.134
	5.8-<6.0	0.000	0.000	0.000	0.000	0.000	0.000	0.000	0.000	0.000	0.000	0.000	0.000	0.000	0.000

R5 Events

		Incident Energy/MeV													
		0.6	0.8	1.0	1.2	1.4	1.6	1.8	2.0	2.2	2.4	2.6	2.8	3.0	3.2
Detected Energy/MeV	0-<0.2	0.000	0.000	0.000	0.000	0.000	0.000	0.000	0.000	0.000	0.000	0.000	0.000	0.000	0.000
	0.2-<0.4	0.000	0.000	0.000	0.000	0.000	0.000	0.000	0.000	0.000	0.000	0.000	0.000	0.000	0.000
	0.4-<0.6	0.000	0.000	0.000	0.000	0.000	0.000	0.000	0.000	0.000	0.000	0.000	0.000	0.000	0.000
	0.6-<0.8	0.000	0.000	0.000	0.000	0.000	0.000	0.000	0.000	0.000	0.000	0.000	0.000	0.000	0.000
	0.8-<1.0	0.000	0.000	0.000	0.000	0.000	0.000	0.000	0.000	0.000	0.000	0.000	0.000	0.000	0.000
	1.0-<1.2	0.000	0.000	0.000	0.000	0.000	0.000	0.000	0.000	0.000	0.000	0.000	0.000	0.000	0.000
	1.2-<1.4	0.000	0.000	0.000	0.000	0.000	0.000	0.000	0.000	0.000	0.000	0.000	0.000	0.000	0.000
	1.4-<1.6	0.000	0.000	0.000	0.000	0.000	0.000	0.000	0.000	0.000	0.000	0.000	0.000	0.000	0.000
	1.6-<1.8	0.000	0.000	0.000	0.000	0.000	0.000	0.000	0.000	0.000	0.000	0.000	0.000	0.000	0.000
	1.8-<2.0	0.000	0.000	0.000	0.000	0.000	0.000	0.000	0.072	0.000	0.000	0.000	0.000	0.000	0.000
	2.0-<2.2	0.000	0.000	0.000	0.000	0.000	0.000	0.000	0.000	0.000	0.000	0.000	0.000	0.000	0.000
	2.2-<2.4	0.000	0.000	0.000	0.000	0.000	0.000	0.000	0.000	0.000	0.000	0.001	0.000	0.000	0.000
	2.4-<2.6	0.000	0.000	0.000	0.000	0.000	0.000	0.000	0.000	0.000	0.000	0.011	0.011	0.000	0.010
	2.6-<2.8	0.000	0.000	0.000	0.000	0.000	0.000	0.000	0.000	0.000	0.000	0.000	0.010	0.067	0.029
	2.8-<3.0	0.000	0.000	0.000	0.000	0.000	0.000	0.000	0.000	0.000	0.000	0.000	0.000	0.407	0.000
	3.0-<3.2	0.000	0.000	0.000	0.000	0.000	0.000	0.000	0.000	0.000	0.000	0.000	0.000	0.000	0.412
	3.2-<3.4	0.000	0.000	0.000	0.000	0.000	0.000	0.000	0.000	0.000	0.000	0.000	0.000	0.000	0.000
	3.4-<3.6	0.000	0.000	0.000	0.000	0.000	0.000	0.000	0.000	0.000	0.000	0.000	0.000	0.000	0.000
	3.6-<3.8	0.000	0.000	0.000	0.000	0.000	0.000	0.000	0.000	0.000	0.000	0.000	0.000	0.000	0.000
	3.8<-3.0	0.000	0.000	0.000	0.000	0.000	0.000	0.000	0.000	0.000	0.000	0.000	0.000	0.000	0.000
	4.0-<4.2	0.000	0.000	0.000	0.000	0.000	0.000	0.000	0.000	0.000	0.000	0.000	0.000	0.000	0.000
	4.2-<4.4	0.000	0.000	0.000	0.000	0.000	0.000	0.000	0.000	0.000	0.000	0.000	0.000	0.000	0.000
	4.4-<4.6	0.000	0.000	0.000	0.000	0.000	0.000	0.000	0.000	0.000	0.000	0.000	0.000	0.000	0.000
	4.6-<4.8	0.000	0.000	0.000	0.000	0.000	0.000	0.000	0.000	0.000	0.000	0.000	0.000	0.000	0.000
	4.8-<5.0	0.000	0.000	0.000	0.000	0.000	0.000	0.000	0.000	0.000	0.000	0.000	0.000	0.000	0.000

	4.0-<5.2	0.000	0.000	0.000	0.000	0.000	0.000	0.000	0.000	0.000	0.000	0.000	0.000	0.000	0.000
	5.2-<5.4	0.000	0.000	0.000	0.000	0.000	0.000	0.000	0.000	0.000	0.000	0.000	0.000	0.000	0.000
	5.4-<5.6	0.000	0.000	0.000	0.000	0.000	0.000	0.000	0.000	0.000	0.000	0.000	0.000	0.000	0.000
	5.6-<5.8	0.000	0.000	0.000	0.000	0.000	0.000	0.000	0.000	0.000	0.000	0.000	0.000	0.000	0.000
	5.8-<6.0	0.000	0.000	0.000	0.000	0.000	0.000	0.000	0.000	0.000	0.000	0.000	0.000	0.000	0.000

		Incident Energy/MeV													
		3.4	3.6	3.8	4.0	4.2	4.4	4.6	4.8	5.0	5.2	5.4	5.6	5.8	6.0
Detected Energy/MeV	0-<0.2	0.000	0.000	0.000	0.000	0.000	0.000	0.000	0.000	0.000	0.000	0.000	0.000	0.000	0.000
	0.2-<0.4	0.000	0.000	0.000	0.000	0.000	0.000	0.000	0.000	0.000	0.000	0.000	0.000	0.000	0.000
	0.4-<0.6	0.000	0.000	0.000	0.000	0.000	0.000	0.000	0.000	0.000	0.000	0.000	0.000	0.000	0.000
	0.6-<0.8	0.000	0.000	0.000	0.000	0.000	0.000	0.000	0.000	0.000	0.000	0.000	0.000	0.000	0.000
	0.8-<1.0	0.000	0.000	0.000	0.000	0.000	0.000	0.000	0.000	0.000	0.000	0.000	0.000	0.000	0.000
	1.0-<1.2	0.000	0.000	0.000	0.000	0.000	0.000	0.000	0.000	0.000	0.000	0.000	0.000	0.000	0.000
	1.2-<1.4	0.000	0.000	0.000	0.000	0.000	0.000	0.000	0.000	0.000	0.000	0.000	0.000	0.000	0.000
	1.4-<1.6	0.000	0.000	0.000	0.000	0.000	0.000	0.000	0.000	0.000	0.000	0.000	0.000	0.000	0.000
	1.6-<1.8	0.000	0.000	0.000	0.000	0.000	0.000	0.000	0.000	0.000	0.000	0.000	0.000	0.000	0.000
	1.8-<2.0	0.000	0.001	0.000	0.000	0.000	0.000	0.000	0.000	0.000	0.000	0.000	0.000	0.000	0.000
	2.0-<2.2	0.000	0.010	0.000	0.000	0.000	0.001	0.000	0.000	0.000	0.000	0.000	0.000	0.000	0.000
	2.2-<2.4	0.000	0.010	0.000	0.000	0.000	0.000	0.001	0.000	0.000	0.047	0.000	0.000	0.000	0.000
	2.4-<2.6	0.010	0.001	0.000	0.001	0.000	0.000	0.000	0.000	0.010	0.000	0.011	0.019	0.000	0.057
	2.6-<2.8	0.029	0.001	0.029	0.000	0.090	0.067	0.072	0.038	0.095	0.029	0.019	0.000	0.086	0.029
	2.8-<3.0	0.000	0.000	0.067	0.029	0.010	0.049	0.038	0.102	0.010	0.066	0.011	0.040	0.011	0.150
	3.0-<3.2	0.412	0.069	0.076	0.000	0.000	0.092	0.119	0.117	0.001	0.020	0.039	0.029	0.019	0.077
	3.2-<3.4	0.000	1.396	0.301	0.141	0.047	0.087	0.030	0.076	0.020	0.096	0.087	0.116	0.060	0.029
	3.4-<3.6	0.000	0.000	1.032	0.171	0.151	0.087	0.041	0.011	0.031	0.021	0.089	0.050	0.172	0.158
	3.6-<3.8	0.000	0.000	0.000	1.565	0.127	0.070	0.031	0.058	0.059	0.123	0.039	0.125	0.076	0.097
	3.8<-3.0	0.000	0.000	0.000	0.000	1.438	0.290	0.171	0.338	0.001	0.144	0.011	0.067	0.117	0.001
	4.0-<4.2	0.000	0.000	0.000	0.000	0.000	1.802	0.107	0.165	0.041	0.060	0.089	0.022	0.136	0.031
	4.2-<4.4	0.000	0.000	0.000	0.000	0.000	0.000	1.254	0.383	0.126	0.126	0.108	0.039	0.110	0.088
	4.4-<4.6	0.000	0.000	0.000	0.000	0.000	0.000	0.000	1.719	0.174	0.072	0.087	0.079	0.142	0.192
	4.6-<4.8	0.000	0.000	0.000	0.000	0.000	0.000	0.000	0.000	1.154	0.107	0.097	0.000	0.106	0.141
	4.8-<5.0	0.000	0.000	0.000	0.000	0.000	0.000	0.000	0.000	0.000	0.539	0.247	0.088	0.220	0.127
	4.0-<5.2	0.000	0.000	0.000	0.000	0.000	0.000	0.000	0.000	0.000	0.000	0.678	0.230	0.101	0.040

	5.2-<5.4	0.000	0.000	0.000	0.000	0.000	0.000	0.000	0.000	0.000	0.000	0.000	0.656	0.078	0.145
	5.4-<5.6	0.000	0.000	0.000	0.000	0.000	0.000	0.000	0.000	0.000	0.000	0.000	0.000	0.341	0.152
	5.6-<5.8	0.000	0.000	0.000	0.000	0.000	0.000	0.000	0.000	0.000	0.000	0.000	0.000	0.000	0.447
	5.8-<6.0	0.000	0.000	0.000	0.000	0.000	0.000	0.000	0.000	0.000	0.000	0.000	0.000	0.000	0.000